Pergamon

International Journal of Plasticity, Vol. 12, No. 4, pp. 451–479, 1996

0749-6419/96 $15.00 + .00

S0749-6419(95)00016-2

PARAMETER IDENTIFICATION FOR VISCOPLASTIC MODELS BASED ON ANALYTICAL DERIVATIVES OF A LEAST-SQUARES FUNCTIONAL AND STABILITY INVESTIGATIONS

Rolf Mahnken and Erwin Stein

Institut für Baumechanik and Numerische Mechanik, University of Hannover, Applestrasse 9a, 30167 Hannover, Germany

(Received in final revised form 6 October 1995)

Abstract—In this work a unified strategy for identification of material parameters of viscoplastic constitutive equations from uniaxial test data is presented. Gradient-based descent methods (e.g. Gauss–Newton method, Quasi–Newton method) are used for minimization of a least-squares functional, thus requiring the associative gradient. The corresponding sensitivity analysis is explained in detail, where as a main result a recursion formula is obtained. Furthermore, the stability of the numerical results for the material parameters is investigated by use of the eigenvalues for the Hessian of the least-squares functional. Numerical examples are presented in the context of monotonic and cyclic loading. In particular, comparative results with a genetic algorithm reflect the efficiency of our strategy with respect to execution time, and we study the effect of perturbations of the experimental data on the stability of the parameters. In one example we demonstrate how possible instabilities can be circumvented by a regularization of the basic least-squares functional. Copyright © 1966 Elsevier Science Ltd

I. INTRODUCTION

The design of engineering structures — e.g. in the context of the finite element method — requires mathematical models capable of accurately predicting short-term and long-term deformations and stresses due to mechanical and thermal loading. In general, these models are given as a set of differential equations that consider transient and steady-state creep, cyclic hardening and softening, Bauschinger effect, rate effects, temperature effects, isotropic and discontinuous damage development, etc. Apart from different quantities such as stresses, temperatures, internal variables, etc., they also depend on material parameters, thus characterizing the specific material. In general, identification of these parameters, which in mathematical terminology is an inverse problem, is based on experimental data. The loading program in the experiment is characterized by controlled strains or strain rates, controlled stresses or stress rates or a combination of these, respectively.

In some cases identification of parameters becomes very simple. Considering Nortons law $\dot{\varepsilon} = (\sigma/K)^N$, the two coefficients K and N can be obtained from the graph $\ln(\sigma)$ versus $\ln(\dot{\varepsilon})$ by hand fitting of the results of secondary creep (see e.g. Lemaitre and Chaboche [1990], p. 284). For more complex situations it is possible to extend this *mechanistic approach* in a systematic manner. Basically, this strategy involves (1)

physical and phenomenological interpretations of the constants in relation to standard uniaxial, ideal tests; (2) distinguishing between different effects, such as kinematic hardening, recovery and damage effects separately in the experimental data; (3) certain *ad hoc* assumptions (e.g. neglecting elastic parts of strains); (4) evaluating the parameters in a sequential manner. Here the data from one test are used to evaluate one or two parameters and these parameters are then used as input, along with data from other tests to evaluate more parameters. In this way a method is proposed by Huang and Khan [1992] to determine the parameters of the model of Bodner and Partom [1975] based on different stress–strain curves. Furthermore, Krieg *et al.* [1987] evaluated parameters based on certain strain- and stress-controlled experiments for a set of constitutive equations involving kinematic and isotropic hardening. Here, the critical *ad hoc* assumption is made that in a stress relaxation test a constant back stress is assumed.

Following Senseny *et al.* [1993] the above mechanistic approach suffers from the following drawbacks:

- The ideal test conditions often cannot be realized in the laboratory, e.g. instantaneous change in inelastic strain rate (see also Huang and Khan [1992]).
- As a consequence of the parameters being evaluated sequentially, values of parameters may depend upon the order in which they were determined.
- The associative *ad hoc* assumptions may be unrealistic.

In this paper we will consider parameter identification as an optimization problem, which allows for a *simultaneous* determination of the parameters. The corresponding objective function, basically, is of least-squares type, thus minimizing the discrepancies between measured quantities and computed quantities.

Concerning the choice of the optimization strategy, very often a genetic algorithm is preferred in practice because of its versatility; see, for example, Müller and Hartmann [1989]; Kublik and Steck [1992]. However, as a major drawback the method is very time-consuming, since in general many function evaluations (several hundred thousand) are necessary. Thus, for reasons of efficiency, we will apply an optimization strategy based on gradient evaluations. Furthermore, we will present a unified strategy for analytical determination of the associative gradient of the least-squares functional for a certain class of material models with internal variables.

Another object of this paper is to discuss and investigate the stability of the results for the identification process, since instability is a typical feature of inverse problems (see Baumeister [1987]; Morozow [1984]; Banks and Kunisch [1989]; Louis [1989]). To this end two indicators are investigated: we examine the eigenvalues of the Hessian of the least-squares functional and we study the effect of perturbation of the experimental data on the parameters. Furthermore, for the case of numerically instable results we introduce a regularization due to Tikhonov, which can be interpreted as an enhancement of the basic least-squares functional by adequate model information.

This paper is organized as follows: In Section II we summarize some specific examples of constitutive models, i.e. the models due to Chaboche [1977], Bodner and Partom [1975] and Steck [1985]. Then we give a brief formulation of the direct and the inverse problem in stress-controlled one-dimensional viscoplasticity. In Sections III and IV the discretized formulations of the direct problem and the inverse problem, respectively, are presented. We discuss solution strategies based on linearization procedures where, in particular, a recursion formula is obtained for the inverse problem.

Section V outlines the optimization strategies based on gradient evaluations. In particular we address some specific issues in the context of an algorithm due to Bertsekas [1982], such as indefinite Hessians, Line-Search strategies, scaling and use of different iteration matrices. In Section VI numerical results are performed in the context of monotonic and cyclic uniaxial tension and compression tests. In particular we demonstrate that numerical instabilities, or even nonuniqueness, for the identification process may occur for the Chaboche model in the case of monotonic loading. Furthermore, comparative results with a genetic algorithm demonstrate the efficiency of our strategy with respect to execution time, and we will show how possible instabilities can be circumvented by a regularization of the basic least-squares functional.

II. BASIC CONCEPTS

II.1 *Mathematical modeling of uniaxial viscoplastic problems*

In this section we describe the basic equations of one-dimensional viscoplastic constitutive theory. Concerning its multiaxial formulation we refer to standard references (see e.g. Miller [1987], Lemaitre and Chaboche [1990]). The theory in its present form assumes small-order isothermal deformations (less than 5%). The strains — or the strain rates, respectively — are decomposed additively into elastic and inelastic components, of which the latter is taken to be volume preserving.

Let $I = [0, T]$ be the time interval of interest. The uniaxial stress is designated by $\sigma = \sigma_{11}$: $I \to \mathbb{R}$, while ε^{el} and ε^{in}: $I \to \mathbb{R}$, are the elastic and inelastic parts of the small strain tensor components ε_{ij}^{in} and ε_{ij}^{el}, respectively. Thus we have

$$\varepsilon = \varepsilon^{el} + \varepsilon^{in}, \tag{1}$$

where

$$\varepsilon^{el} = \frac{1}{E}\sigma \tag{2}$$

is the constitutive equation for the elastic part, and E is the elastic modulus.
Concerning the inelastic part of (1), constitutive equations for ε^{in}, typically, are given in rate form accompanied by a set of equations for n_q internal — nonmeasurable — variables $\mathbf{q} \in \mathbb{R}^{n_q}$

$$\boxed{\begin{aligned} \dot{\varepsilon}^{in} &= \hat{\dot{\varepsilon}}^{in}(\sigma, \mathbf{q}, \theta, \varepsilon^{in}, \ldots; \kappa) \\ \dot{\mathbf{q}} &= \hat{\dot{\mathbf{q}}}(\sigma, \mathbf{q}, \theta, \varepsilon^{in}, \ldots; \kappa) \end{aligned}} \tag{3}$$

Here, additionally, we defined the temperature θ, and $\kappa \in \mathbb{R}^m$ is a vector of m material parameters.

There exist a great variety of constitutive relations in the literature according to the above skeletal structure (3) (see e.g. Miller [1987], Lemaitre and Chaboche [1990] and references therein). Many approaches intend to provide for a number of different characteristic effects, such as strain rate dependent plastic flow, creep or stress relaxation. In doing so a yield criterion with the inherent specification of loading and unloading conditions as in time-independent classical plasticity is not needed. The resulting equations are currently referred to as "unified models". The internal variables, in principle, are argued for macroscopic or microscopic reasons depending on the basic conception.

Three representative examples of (3) are considered in this paper: the models of Chaboche [1977], Bodner and Partom [1975] and Steck [1985] (see also Kublik and Steck [1992]). The specific formulations of the three models are summarized in Table 1.

It can be seen that the Chaboche model has $n_q = 2$ internal variables, which may be viewed as the minimum for cyclic loading (Swearengen & Holbrook [1985]). A yield surface F is present in the model, such that for $F < 0$ elastic behaviour takes place. As a major difference to constitutive laws in plasticity we may have $F > 0$, so that F can also be viewed as an over-stress. The internal variable R accounts for isotropic hardening, and the back-stress term $\alpha = \alpha_{11}$ is incorporated to permit description of material response to unloading, including the Bauschinger effect. Note, that both (stress-like) internal variables, R and α, consist of a hardening term and a recovery term. The constitutive equation for α may be viewed as a modification of the linear Prager [1949] rule.

The Bodner and Partom [1975] model involves one internal variable for isotropic hardening. Note, that in Table 1 we cited the original formulation of Bodner and Partom [1975]. In more recent works, e.g. Bodner [1987], it was slightly modified, e.g. the factor $(n' + 1)/n'$ was left out. Bodner [1987] describes a mechanistic approach for identification of the model. In this way the variable D_0 is fixed for a strain rate range. From Bodner [1987], p. 286, it may be interpreted as the maximum value of strain rate in shear, and its physical existence can be argued on the grounds of dislocation theory. On this basis, values for the maximum value of D_0 are summarized in Table 2 as recommended by Bodner [1987]. The internal variable Z is related to the total

Table 1. Uniaxial formulation of three specific examples for constitutive equations. In Steck's model R is a gas constant and U_0 is the activation energy for self diffusion

Chaboche [1977]

$$\dot{\varepsilon}^{in} = \begin{cases} \left(\frac{F}{K'}\right)^{n'} \operatorname{sgn}(\sigma - \alpha), & \text{if } F > 0 \\ 0, & \text{else} \end{cases}$$

$\dot{R} = b(q - R)\,\dot{\varepsilon}^{in}\,\operatorname{sgn}(\dot{\varepsilon}^{in})$ (isotropic hardening)
$\dot{\alpha} = c(\gamma - \alpha \operatorname{sgn}(\dot{\varepsilon}^{in}))\,\dot{\varepsilon}^{in}$ (kinematic hardening)
$F = (\sigma - \alpha)\operatorname{sgn}(\sigma - \alpha) - R - k'$ (over–stress)
seven material parameters: $\kappa = [n', K', b, q, c, \gamma, k']^T$
two internal variables: R, α

Bodner and Partom [1975]

$$\dot{\varepsilon}^{in} = \frac{2}{\sqrt{3}} D_0 \exp\left[-\frac{1}{2}\frac{n'+1}{n'}\left(\frac{Z}{\sigma}\right)^{2n'}\right] \operatorname{sgn}(\sigma)$$

$\dot{Z} = \frac{m'}{Z_0}(Z_1 - Z)\sigma\,\dot{\varepsilon}^{in}$ (isotropic hardening)

five material parameters: $\kappa = [D_0, Z_0 = Z(t = 0), Z_1, n', m']^T$
one internal parameter: Z

Steck [1985]

$$\dot{\varepsilon}^{in} = \lambda' c_1 \exp\left[-\left(1 - \frac{\alpha - 1}{\kappa'}\frac{U_0}{R\theta}\right)\right] \times \left(2\sinh\left(\frac{\Delta V}{R\theta}\sigma\right)\right)^{1+\frac{1}{\kappa'}} \exp\left(-\frac{F}{R\theta}\right)$$

$$\dot{F} = \frac{1}{\lambda'}\dot{\varepsilon}^{in} - c_2 \exp\left[-\frac{\alpha U_0 - \beta F}{R\theta}\right]$$ (isotropic hardening)

seven material parameters: $\kappa = [\lambda', \Delta V, c_1, c_2, \alpha, \beta, \kappa']^T$
one internal parameter: F

Table 2. Values for D_0 of the Bodner and Partom model recommended by Bodner [1987]

$\dot{\varepsilon}^{in}$	<10	$10–10^3$	$>10^3$
D_0 [s^{-1}]	10^4	10^6	10^7

dislocation density. Note as a special feature of the model, that the initial value $Z_0 = Z\ (t = 0)$ is regarded as a material parameter.

The stochastic model due to Steck [1985] (see also Kublik & Steck [1992]) is based on the observation that deformation can be described by a movement of dislocations. Therefore, flow units are introduced representing, for example, dislocations or dislocation packages. It is assumed that each flow unit is situated in a class of an internal barrier energy formed by solute atoms, grain boundaries, dispersed particles or entangled dislocations. If they step into a class of higher energy, this results in hardening; if they step into a class of lower energy, recovery is attained. Each of these processes is described by a transition probability. In the original model of Steck [1985] the flow units are located in a discrete number of energy classes. In Kublik and Steck [1992] a reduction of all classes of internal barrier-energy to one is proposed. The resulting model is the stochastic mean-value model, with one internal variable F describing isotropic hardening, which is correlated to the mean internal barrier energy. A modification of the model to account for cyclic deformation is described in Schlums and Steck [1992]. For parameter determination there is no mechanistic approach. In Kublik [1992], a least-squares minimization technique is applied, whereby the resulting objective functional is minimized with a genetic algorithm.

Lastly, in order to formulate the complete initial value problem, we assume that initial conditions

$$\sigma(t = 0) = \sigma_0, \quad \varepsilon^{in}(t = 0) = \varepsilon_0^{in}, \quad \mathbf{q}(t = 0) = \mathbf{q}_0 \tag{4}$$

are given.

II.2 *The direct problem*

Let us assume a prescribed temperature $\theta(t)$ and stress distribution $\sigma(t)$, $t \in I$ in a stress-controlled experiment. Let U be the solution space for the strain trajectory $\varepsilon(\bullet;\ \kappa)$ of the above initial-value problem (1)–(4). Then, assuming given material parameters $\kappa \in \mathbb{R}^m$, along with the above initial-value problem (1)–(4), this characterizes the *direct problem* for the strains as

$$\boxed{\kappa \mapsto \varepsilon(\bullet;\ \kappa); \quad \mathbb{R}^m \to U,} \tag{5}$$

which in general can be solved in a *forward calculation.*

II.3 *The inverse problem*

Let $\bar{U}$ denote an observation space, and let $\bar{\varepsilon} \in \bar{U}$ denote given data from experiments. To account for the possibility that only incomplete data are available, we introduce an observation operator $\mathcal{M}$ mapping the strain trajectory to points $\mathcal{M}\varepsilon(\bullet;\ \kappa)$ in the observation space $\bar{U}$ (Banks & Kunisch [1989], p. 54). Then, the objective is to solve the *inverse problem*

$$\boxed{\text{Find } \kappa\text{: } \mathcal{M}\varepsilon(\bullet;\, \kappa) = \bar{\varepsilon} \text{ for given } \bar{\varepsilon} \in \bar{U}} \tag{6}$$

in a *backward calculation*. It is well known that the above problem is ill-posed in the sense of Hadamard [1923], since in general no solution exists. Therefore, the backward calculation is replaced by an *optimal approach strategy*; that is, we consider the parameter identification as an optimization problem:

$$\boxed{f(\kappa) := \tfrac{1}{2}\|\mathcal{M}\varepsilon(\bullet;\, \kappa) - \bar{\varepsilon}\|^2_{\bar{U}} \to \min_{\kappa \in \mathbb{R}^m}} \tag{7}$$

Remarks

1. In practice observations are given at discrete times $\{t_i\}_{i=1}^{n_{\text{dat}}} \subset I$. Then, for the case of one experiment, the observation space is $\bar{U} = \mathbb{R}^{n_{\text{dat}}}$, i.e. $\bar{\varepsilon} = [\bar{\varepsilon}_1, \ldots, \bar{\varepsilon}_{n_{\text{dat}}}]^T$, where $\bar{\varepsilon}_i = \bar{\varepsilon}(t_i)$, $i = 1 \ldots, n_{\text{dat}}$. Furthermore, the observation operator is defined by $\mathcal{M}\varepsilon(\bullet;\, \kappa) = [\varepsilon_1(\kappa), \ldots, \varepsilon_{n_{\text{dat}}}(\kappa)]^T =: \varepsilon(\kappa)$, where $\varepsilon_i(\kappa) = \varepsilon(t_i;\, \kappa)$, $i = 1, \ldots, n_{\text{dat}}$. Consequently, the discrete least-squares analogue of the functional in problem (7) is written as

$$\boxed{f(\kappa) = \tfrac{1}{2}\|\varepsilon(\kappa) - \bar{\varepsilon}\|^2_2.} \tag{8}$$

For the case of more than one experiment, e.g. at different temperatures, the above functional has to be modified accordingly.

2. Let us comment on two different type of errors: For this purpose let $\hat{\varepsilon}(t)$ $t \in I$ denote the *true state* corresponding to a process with given distribution $(\sigma(t),\ \theta(t),\ t \in I$. Then, even for a correct parameter κ^* the following situations may arise

- $\mathcal{M}\hat{\varepsilon}(\bullet) \neq \bar{\varepsilon}$ due to *measurement errors*
- $\hat{\varepsilon}(\bullet) \neq \varepsilon(\bullet;\, \kappa^*)$ due to *model errors*

3. In many situations, the problem (7), though well-posed, may lead to numerically *instable solutions*, i.e. small variations of $\bar{\varepsilon}$ may lead to large variations of the parameters κ. These difficulties are caused, e.g. if the material model has (too many) parameters, which yield (almost) linearly dependencies within the model, or if the experiment is inadequate in the sense that some parts of the model are not properly "activated".

In some cases even *nonuniqueness* of the solution is possible: For example, considering the Steck model of Table 1, this occurs for the case of isothermal identification, since then a dependence of three parameters is present (see Mahnken & Stein [1994a]). Furthermore, considering the Chaboche model of Table 1, the evolution equations for the isotropic hardening and the kinematic hardening qualitatively become identical for monoton loading as long as $\sigma > \alpha$, since $\operatorname{sgn}(\dot{\varepsilon}^{\text{in}}) = 1$ in this case. Then various combinations of b, q and c, γ, respectively, may lead to the *same* solution of the direct problem. For the inverse problem it follows that an infinite number of solution exists; i.e. the results are not unique. Consequently, at least cyclic loading is necessary in order to activate the differences of both evolution equations of the model. In other words, *the input for the identification process has to be sufficiently rich such that the output is persistent excited* (Baumeister, private communication).

4. As a consequence of the above Remark 3 it is strongly recommended to study the effect of perturbations of the experimental data on the parameters. This may indicate possible instabilities of the identification process.

5. A mathematical tool suitable for overcoming possible numerical instabilities is a regularization of the functional in (8); this leads to the more general problem

$$f_\gamma(\boldsymbol{\kappa}) = \tfrac{1}{2}\|\mathbf{B}_\delta(\boldsymbol{\varepsilon}(\boldsymbol{\kappa}) - \bar{\boldsymbol{\varepsilon}})\|_2^2 + \tfrac{\gamma}{2}\|\mathbf{B}_\mu(\boldsymbol{\kappa} - \bar{\boldsymbol{\kappa}})\|_2^2 \to \min_{\boldsymbol{\kappa} \in \mathbb{R}^m} \tag{9}$$

Here the matrices $\mathbf{B}_\delta \in \mathbb{R}^{n\text{dat}} \times \mathbb{R}^{n\text{dat}}$ and $\mathbf{B}_\mu \in \mathbb{R}^m \times \mathbb{R}^m$, the scalar $\gamma \in \mathbb{R}^+$ and the *a priori* parameters $\bar{\boldsymbol{\kappa}} \in \mathbb{R}^m$ are *regularization parameters* (Morozow [1984]; Baumeister [1987]; Louis [1989]). Note that the first part of the functional in problem (9) is also obtained when considering parameter identification based on statistical investigations in the context of a maximum likelihood method, in order to account for measurement errors. It is noteworthy that the r.h.s. of the functional is also related to the Bayesian estimation (Bard [1974]; Pugachew [1984]). The above function provides the opportunity to include physical interpretation of some parameters (obtained, for example, by a mechanistic approach mentioned in Section I) into the optimization process, if numerical instabilities occur. However, a systematic concept for determination of the regularization parameters in the context of parameter identification for viscoplastic material models so far is not available.

6. The representation above — and in the forthcoming sections — is based on stress-controlled experiments. Of course, analogous arguments hold for the complementary tests, i.e. strain-controlled experiments, where experimental data are given for stresses $\bar{\sigma}(t)$, $t \in I$. Furthermore, in an analogous way a combination of stress- and strain-controlled experiments is treated. Note, that identical results for stress- and strain-controlled experiments can only be obtained if the model at hand can represent the real data without measurement errors, i.e. the model errors must also be zero. Of course, these conditions are only necessary but not sufficient for a unique solution of the corresponding inverse problem.

III. NUMERICAL SOLUTION OF THE DIRECT PROBLEM

III.1 *Time integration scheme*

In this section we present a systematic approach for solution of the direct problem (1–4). The resulting equations will be the point of departure for numerical solution of the corresponding inverse problem in the next section.

We define N as the number of time steps $\Delta t_k = t_k - t_{k-1}$, $k = 1, \ldots, N$, $t_0 = 0$, $t_N = T$. Using the second order midpoint-rule at each time step, we have the relations

$$\varepsilon_k = \varepsilon_{k-1} + \Delta t_k \dot{\varepsilon}^{\text{in}}_{k-1/2} + \Delta \varepsilon^{\text{el}}_{k-1} \tag{10}$$

$$\mathbf{q}_k = \mathbf{q}_{k-1} + \Delta t_k \dot{\mathbf{q}}_{k-1/2}, \tag{11}$$

where we applied the notation

$$\dot{\varepsilon}^{\text{in}}_{k-1/2} := \dot{\varepsilon}^{\text{in}}(1/2(\sigma_{k-1} + \sigma_k),\ 1/2(\mathbf{q}_{k-1} + \mathbf{q}_k),\ \ldots;\boldsymbol{\kappa}) \tag{12}$$

$$\dot{\mathbf{q}}_{k-1/2} := \dot{\mathbf{q}}(1/2(\sigma_{k-1} + \sigma_k),\ 1/2(\mathbf{q}_{k-1} + \mathbf{q}_k),\ \ldots;\boldsymbol{\kappa}) \tag{13}$$

$$\Delta \varepsilon^{\text{el}}_{k-1} := \frac{1}{E}(\sigma_k - \sigma_{k-1}). \tag{14}$$

Since the *state variables* ε_k and $\mathbf{q}_k$ are not known in advance, the following nonlinear system of equations has to be solved at each time step:

$$g_{k,1}(\varepsilon_k, \mathbf{q}_k) := \varepsilon_k - \varepsilon_{k-1} - \Delta t_k \dot{\varepsilon}^{\text{in}}_{k-1/2} - \Delta \varepsilon^{\text{el}}_{k-1} = 0 \tag{15}$$

$$\mathbf{g}_{k,2}(\varepsilon_k, \mathbf{q}_k) := \mathbf{q}_k - \mathbf{q}_{k-1} - \Delta t_k \dot{\mathbf{q}}_{k-1/2} = 0. \tag{16}$$

Defining $\mathbf{G}_k := [g_{k,1}, \mathbf{g}_{k,2}{}^T]^T$ and a vector of *state variables* $\mathbf{Y}_k := [\varepsilon_k, \mathbf{q}_k{}^T]^T$, (15) and (16) may be summarized as

$$\boxed{\mathbf{G}_k(\mathbf{Y}_k) = 0.} \tag{17}$$

In the sequel the relation (17) will be referred to as the *state equation*, describing the state of the state variables $\mathbf{Y}_k := [\varepsilon_k, \mathbf{q}_k^T]^T$ at each time state t_k.

III.2 *Solution strategy*

For solution of problem (17) a Newton method is used according to the iteration scheme

$$\mathbf{Y}_k^{(i+1)} = \mathbf{Y}_k^{(i)} - \alpha^{(i)} [\mathbf{J}_k^{(i)}]^{-1} \mathbf{G}_k^{(i)}, \tag{18}$$

where $\alpha^{(i)}$ is a step-length, determined in a line-search (see, for example, Dennis & Schnabel [1983]; Luenberger [1984]), and

$$\mathbf{J}_k^{(i)} := \left. \frac{\partial \mathbf{G}_k(\mathbf{Y}_k)}{\partial \mathbf{Y}_k} \right|_{\mathbf{Y}_k = \mathbf{Y}_k^{(i)}} \tag{19}$$

is the Jacobian of $\mathbf{G}_k(\mathbf{Y}_k)$. In cases of the Bodner and Partom model the result for $\mathbf{J}_k$ is given in Appendix A. On corresponding results for the stochastic model of Steck we refer to Mahnken and Stein [1994b]. The results of the Chaboche model require some lengthy algebra not reported in this paper.

Remark
For complementary tests of the above situation, i.e. strain-controlled experiments with given distribution $(\varepsilon(t), \theta(t), t \in I)$, basically, the same procedure as described above may be used, by defining $\mathbf{Y}_k := [\sigma_k, \mathbf{q}_k^T]^T$ as the vector of (unknown) state variables at each time step.

IV. NUMERICAL SOLUTION OF THE INVERSE PROBLEM

IV.1 *Discretized formulation*

For reasons of simplicity, in the sequel, we will assume that the discrete values for time integration $\{t_k\}_{k=1}^N \subset I$ and for the experimental data $\{t_k^{\text{exp}}\}_{k=1}^{n_{\text{dat}}} \subset I$ do coincide for both the numerical values $\varepsilon_k = \varepsilon(t_k; \kappa)$ and the observations $\bar{\varepsilon}_k = \bar{\varepsilon}(t_k)$, $k = 1, \ldots, N$. The following considerations can be extended to more complex situations in a straightforward manner.

As noted in Section II.2, parameter identification is treated as minimizing some objective functional $f(\kappa)$ with respect to κ. Additionally, the state equation (17) of the direct problem has to be satisfied at each time step. Therefore, the following optimization problem with constraints is formulated:

$$\boxed{\begin{aligned} f(\boldsymbol{\kappa}, \{\mathbf{Y}_k\}_{k=1}^N) &\to \min_{\boldsymbol{\kappa},\, \{\mathbf{Y}_k\}_{k=1}^N} \\ \mathbf{G}_k(\mathbf{Y}_k) &= \mathbf{0}, \quad k = 1, \ldots, N. \end{aligned}} \tag{20}$$

The unknowns of problem (20) are $\mathbf{Y}_k$, $k = 1, \ldots, N$, and κ_i, $i = 1, \ldots, m$, i.e. the highly nonlinear optimization problem (20) is characterized by its large dimension and many constraints.

IV.2 *Solution strategy*

A very effective solution strategy to problem (20) is applied as follows:

- The material parameters $\boldsymbol{\kappa}$ are regarded as *independent variables*
- The state variables are *dependent variables*, i.e. $\mathbf{Y}_k = \hat{\mathbf{Y}}_k(\boldsymbol{\kappa})$, $k = 1, \ldots, N$.

The resulting optimization problem without constraints is now given by

$$\boxed{\begin{aligned} & f(\boldsymbol{\kappa}, \{\hat{\mathbf{Y}}(\boldsymbol{\kappa})\}_{k=1}^N) \to \min_{k \in \mathbb{R}^m} \\ \text{where } & \{\hat{\mathbf{Y}}_k(\boldsymbol{\kappa})\}_{k=1}^N \quad \text{satisfies} \\ & \mathbf{G}_k(\boldsymbol{\kappa}, \hat{\mathbf{Y}}_k(\boldsymbol{\kappa})) = \mathbf{0}, \quad k = 1, \ldots, N. \end{aligned}} \tag{21}$$

It can be seen that the above strategy reduces the dimension of the optimization problem significantly to $\dim(\boldsymbol{\kappa})$. However, it should be noted that the functions of interest now depend on $\boldsymbol{\kappa}$ both explicitly and implicitly.

As a practical consequence it follows that in an optimization process for the solution of problem (21) a complete analysis for the problems $(21)_2$ has to be carried out for any set of material parameters $\kappa^{(j)}$, $j = 1, 2, \ldots$. A schematic flow chart with a simplified description is shown in Fig. 1. It can be seen that, basically, an outer loop for iteration of the material parameters and an inner loop for iteration of the state variables $\hat{\mathbf{Y}}_k(\kappa^{(j)})$ are required.

Optimization algorithms for problem (21) can be classified into methods which use only function values (e.g. a genetic algorithm, see Schwefel [1977]) and methods which use function values and gradients (e.g. the SQP-method according to Schittkowski [1981] or a projection algorithm due to Bertsekas [1982]). Since, in general, the first kind of method is not efficient due to large number of function evaluations, the second kind is used. Therefore, the gradient of the objective function has to be determined in a *sensitivity analysis.*

IV.3 *First-order sensitivity analysis*

For ease of explanation we consider the least-squares functional

$$f(\boldsymbol{\kappa}) = \frac{1}{2} \sum_{k=1}^{N} (\varepsilon_k(\boldsymbol{\kappa}) - \bar{\varepsilon}_k)^2 \tag{22}$$

without weighting factors. Clearly, the gradient is given by

$$\nabla f(\boldsymbol{\kappa}) = \sum_{k=1}^{N} (\varepsilon_k(\boldsymbol{\kappa}) - \bar{\varepsilon}_k) \frac{\mathrm{d}\varepsilon_k(\boldsymbol{\kappa})}{\mathrm{d}\boldsymbol{\kappa}}, \tag{23}$$

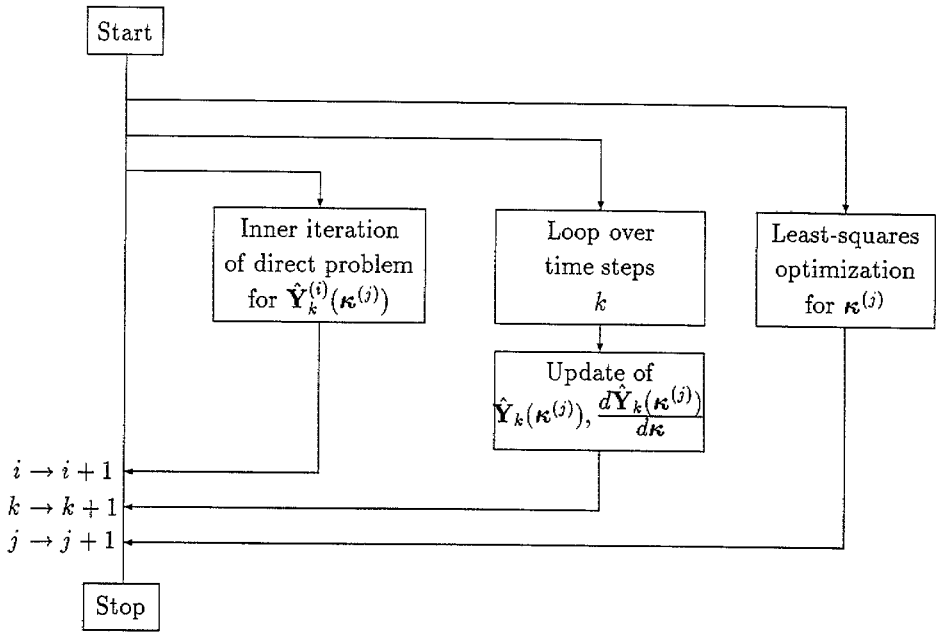

Fig. 1. Schematic flow chart for optimization strategy with outer and inner iteration loops.

and thus, basically, $d\varepsilon_k(\kappa)/d\kappa$ is required. As it will be shown below, a systematic approach for its determination is contained in the calculation of $d\hat{\mathbf{Y}}_k(\kappa)/d\kappa$, where $\hat{\mathbf{Y}}_k(\kappa) = [\varepsilon_k(\kappa), \mathbf{q}_k(\kappa)^T]^T$, as introduced in Section III.1.

The point of departure is the state equation (17) of the direct problem (at the converged state) at the kth time step. It will be regarded as an implicit function; however, the set of arguments is extented by those quantities which depend on the material parameters κ:

$$\hat{\mathbf{G}}_k\,(\kappa,\ \hat{\mathbf{Y}}_k(\kappa),\ \hat{\mathbf{Y}}_{k-1}(\kappa)) = \otimes. \tag{24}$$

For this expression the total differential is given by

$$\frac{d\hat{\mathbf{G}}_k}{d\kappa} = \frac{\partial\hat{\mathbf{G}}_k}{\partial\kappa} + \frac{\partial\hat{\mathbf{G}}_k}{\partial\hat{\mathbf{Y}}_k}\frac{d\hat{\mathbf{Y}}_k}{d\kappa} + \frac{\partial\hat{\mathbf{G}}_k}{\partial\hat{\mathbf{Y}}_{k-1}}\frac{d\hat{\mathbf{Y}}_{k-1}}{d\kappa} = \mathbf{0}, \tag{25}$$

and the unknown quantities are obtained by solution of the following linear system of equations:

$$\boxed{\frac{d\hat{\mathbf{Y}}_k}{d\kappa} = -\underbrace{\left[\frac{\partial\hat{\mathbf{G}}_k}{\partial\hat{\mathbf{Y}}_k}\right]^{-1}}_{1}\left(\underbrace{\frac{\partial\hat{\mathbf{G}}_k}{\partial\kappa}}_{2} + \underbrace{\frac{\partial\hat{\mathbf{G}}_k}{\partial\hat{\mathbf{Y}}_{k-1}}}_{3}\underbrace{\frac{d\hat{\mathbf{Y}}_{k-1}}{\partial\kappa}}_{4}\right)} \tag{26}$$

From the above expression it can be seen that partial derivatives of the state equation (24) with respect to κ, $\hat{\mathbf{Y}}_k$, $\hat{\mathbf{Y}}_{k-1}$ are required. Concerning terms 1–4, the following remarks are noteworthy:

Term 1: This term is identical to the Jacobian $\mathbf{J}_k$ defined in (19).

Term 2: For this term the partial derivatives of the function $\hat{\mathbf{G}}_k$ with respect to the material parameters κ are required.

Term 3: Note the simple relation

$$\frac{\partial \hat{\mathbf{G}}_k}{\partial \hat{\mathbf{Y}}_{k-1}} = \frac{\partial \hat{\mathbf{G}}_k}{\partial \hat{\mathbf{Y}}_k} - 2\mathbf{I}, \tag{27}$$

which holds if the midpoint rule is applied for integration of the direct problem.

Term 4: This term is adopted from the previous time step. Thus it can be seen, that the sensitivity essentially yields a *recursion formula* for $\mathrm{d}\hat{\mathbf{Y}}_k/\mathrm{d}\kappa$. It is not necessary to take into account results from time steps before the previous time step.

Further Remarks

1. As mentioned before, partial differentials of the function $\hat{\mathbf{G}}_k$ with respect to the variables κ, $\hat{\mathbf{Y}}_k$, $\hat{\mathbf{Y}}_{k-1}$ have to be provided. In the case of the Bodner and Partom model of Table 1, the results are given in Appendix A. For the stochastic model of Steck we refer to Mahnken and Stein [1994b]. The analysis for the Chaboche model involves some extensive algebra not reported in this paper.

2. The fact that the sensitivity analysis yields a recursion formula can be exploited in the numerical computation, when solving the direct problem. To this end, the gradient is calculated *simultaneously* to the step-by-step computation of the direct problem. In doing so an update of both the state variables $\hat{\mathbf{Y}}_k(\kappa)$ and its derivatives $\mathrm{d}\hat{\mathbf{Y}}_k(\kappa)/\mathrm{d}\kappa$ becomes necessary at the converged state of each time step (see Fig. 1). Thus, we avoid storing results for $\mathrm{d}\hat{\mathbf{Y}}_k(\kappa)/\mathrm{d}\kappa$ at all time steps.

IV.4 *Second-order sensitivity analysis*

As in the previous section, the point of departure will be the least-squares function (22). Then, the Hessian of $f(\kappa)$ is derived by differentiation of (23) with respect to κ, i.e.

$$\mathbf{F} := \nabla^2 f(\kappa) = \sum_{k=1}^{N} \left(\frac{\mathrm{d}\varepsilon_k(\kappa)}{\mathrm{d}\kappa} \otimes \frac{\mathrm{d}\varepsilon_k(\kappa)}{\mathrm{d}\kappa} + (\varepsilon_k(\kappa) - \bar{\varepsilon}_k) \frac{\mathrm{d}^2 \varepsilon_k(\kappa)}{\mathrm{d}\kappa \otimes \mathrm{d}\kappa} \right). \tag{28}$$

From the above equation it can be seen, that basically $\mathrm{d}^2\varepsilon_k(\kappa)/\mathrm{d}\kappa \otimes \mathrm{d}\kappa$ is required. In Appendix B we show that, conceptionally, the derivation of this term is similar to the derivation of $\mathrm{d}\varepsilon_k/\mathrm{d}\kappa$ described in the previous section. For this purpose we use (25) as an implicit function and calculate the total differential $\mathrm{d}^2\hat{\mathbf{G}}_k/\mathrm{d}\kappa \otimes \mathrm{d}\kappa$. Then, the resulting system of equations is solved for

$$\frac{\mathrm{d}^2 \hat{\mathbf{Y}}_k(\kappa)}{\mathrm{d}\kappa \otimes \mathrm{d}\kappa} = \left[\frac{\mathrm{d}^2 \varepsilon_k(\kappa)}{\mathrm{d}\kappa \otimes \mathrm{d}\kappa}, \frac{\mathrm{d}^2 \mathbf{q}_k(\kappa)}{\mathrm{d}\kappa \otimes \mathrm{d}\kappa} \right]. \tag{29}$$

Let us make some remarks concerning the Hessian of $f(\kappa)$:

1. Contrary to different applications (e.g. for solution of the direct problem) our own numerical tests showed no advantage of the Hessian as an iteration matrix, unless the starting vector $\kappa^{(j=1)}$ was near the solution vector κ^*. This is mainly because $\mathbf{F}$ is not necessarily positive definite during the iteration process.

2. The Hessian $\mathbf{F}^*$ at the solution point κ^* may be viewed as another indicator for the robustness of the solution vector κ^*, along with the study of perturbation effects proposed in Section II.3. If $\mathbf{F}^*$ is singular (or nearly singular), it may be concluded that, as mentioned before, the material parameters are (almost) linearly dependent or the experiment is inadequate.

3. In the subsequent sections, frequently, the first part of the r.h.s of (28) shall be called the Gauss–Newton matrix, i.e.

$$\mathbf{F}_{\mathrm{GN}} := \sum_{k=1}^{N} \left(\frac{\mathrm{d}\varepsilon_k(\boldsymbol{\kappa})}{\mathrm{d}\boldsymbol{\kappa}} \otimes \frac{\mathrm{d}\varepsilon_k(\boldsymbol{\kappa})}{\mathrm{d}\boldsymbol{\kappa}} \right). \tag{30}$$

It follows, that for zero error $(\varepsilon_k(\boldsymbol{\kappa}^*) - \bar{\varepsilon}_k) = 0$, $k = 1, \ldots, N$, the matrix $\mathbf{F}_{\mathrm{GN}}$ is identical to the Hessian $\mathbf{F}$, while with increasing error also the deviations of both matrices become larger.

V. SOME REMARKS ON DESCENT OPTIMIZATION ALGORITHMS

The iteration scheme of a gradient-based method for solution of the optimization problem (21) reads

$$\boldsymbol{\kappa}^{(j+1)} = \boldsymbol{\kappa}^{(j)} - \alpha^{(j)} \left[\mathbf{H}^{(j)}\right]^{-1} \nabla f(\boldsymbol{\kappa}^{(j)}). \tag{31}$$

Here $\alpha^{(j)}$ is a step-length determined in a line search, which may be based on function evaluations (e.g. Armijo line-search — see, for example, Dennis & Schnabel [1983] and Luenberger [1984]) or gradient evaluations (e.g. pegasus method — see, for example, Engeln-Müllges & Reuter [1988]). The iteration matrix $\mathbf{H}^{(j)}$ is a positive-definite iteration matrix. The following choices seem to be preferable:

$$\begin{aligned} \mathbf{H} &= \mathbf{F}_{\mathrm{GN}} \quad \text{(Gauss–Newton method)} \\ [\mathbf{H}]^{-1} &= \mathbf{H}_{\mathrm{BFGS}} \quad \text{(BFGS method).} \end{aligned} \tag{32}$$

For the specific update formula for $\mathbf{H}_{\mathrm{BFGS}}$, we refer to Dennis and Schnabel [1983] and to the modification of Powell [1977] in order to preserve positive-definiteness (see also Luenberger, p. 448). It is noteworthy that we did numerical tests with the gradient method, i.e. $\mathbf{H}^{(j)} = \mathbf{I}^{m \times m}$, where $\mathbf{I}^{m \times m}$ is the identity; however, this choice gave very poor results with respect to execution time.

Remarks

1. For many problems, lower bounds κ_i^l, $i = 1,\ldots,m$, are given for the material parameters. Thus, the resulting optimization problem reads

$$\begin{aligned} f(\boldsymbol{\kappa}) &\rightarrow \min_{\boldsymbol{\kappa} \in \mathbb{R}^m} \\ \kappa_i &\geq \kappa_i^l, \; i = 1, \ldots, m. \end{aligned} \tag{33}$$

Problems of the above kind may be solved with a projection algorithm of Bertsekas [1982] according to the iteration scheme

$$\boldsymbol{\kappa}^{(j+1)} = \mathcal{P}\left\{\boldsymbol{\kappa}^{(j)} - \alpha^{(j)} \bar{\mathbf{H}}^{(j)} \nabla f(\boldsymbol{\kappa}^{(j)})\right\}. \tag{34}$$

The projection operator $\mathcal{P}$ in (34) is defined as

$$(\mathcal{P}\{\boldsymbol{\kappa}\})_i = \max(\kappa_i, \kappa_i^l) \qquad i = 1, \ldots, m. \tag{35}$$

For the choice of the iteration matrix $\bar{\mathbf{H}}$ we refer to Bertsekas [1982] and Mahnken [1992]. Note, that upper bounds κ_i^u, $i = 1,\ldots, m$, may be treated in an analogous manner.

2. During the iteration process it may occur that the iteration matrix $\mathbf{H}$ is not positive-definite or ill-conditioned, thus preventing an adequate descent direction for the iteration process. In this case a modified Cholesky method due to Gill *et al.* [1981] may be applied; this yields an iteration matrix

$$\hat{\mathbf{H}} = \mathbf{H} + \mathbf{E}. \tag{36}$$

Here, the diagonal matrix $\mathbf{E}$ is chosen, such that $\hat{\mathbf{H}}$ becomes positive-definite. Alternatively, a spectral decomposition of $\mathbf{H}$ may be computed such that

$$\mathbf{H} = \mathbf{Q}^{\mathrm{T}}\mathbf{D}\,\mathbf{Q}. \tag{37}$$

Here $\mathbf{D}$ is a diagonal matrix with eigenvalues of $\mathbf{H}$, and $\mathbf{Q}$ is an orthonormal matrix containing eigenvectors of $\mathbf{H}$ (see, for example, Engeln-Müllges & Reuter [1988]). Note that the evaluation of the eigensystem is not expensive since, in general, the dimension for κ is low. Then, if $\boldsymbol{H}$ is not positive-definite, it is replaced by

$$\hat{\mathbf{H}} = \mathbf{Q}^{\mathrm{T}}\hat{\mathbf{D}}\,\mathbf{Q}, \tag{38}$$

where $\mathrm{diag}[\hat{\mathbf{D}}]_i = \max(\varepsilon, \mathrm{diag}[\mathbf{D}]_i)$, $i = 1, \ldots, m$, and ε is some tolerance (for example, $\varepsilon = 10^{-10}$), see Gill *et al.* [1981].

3. For $\mathbf{H} = \mathbf{F}_{\mathrm{GN}}$ and $\mathbf{E} = \mu_c\mathbf{I}$, $\mu_c > 0$ in (36), the resulting algorithm is known as the *Levenberg–Marquardt* method (Luenberger [1984], p. 227; see also Dennis & Schnabel [1983], p. 227).

4. In the case of the BFGS algorithm, scaling plays an important role for conditioning of the iteration matrix (see, for example, Luenberger [1984], p. 275). In our algorithm, scaling was realized according to

$$f(\bar{\kappa}) \to \min_{\bar{\kappa} \in \mathbb{R}^m}, \qquad \bar{\kappa}_i := \frac{\kappa_i}{\kappa_{s,i}}, \quad i = 1, \ldots, m. \tag{39}$$

where κ_s denotes the *scaling parameters* and $\bar{\kappa}$ is a modified variable. It follows by the chain rule that the corresponding gradient has to modified according to

$$\frac{\mathrm{d}f}{\mathrm{d}\bar{\kappa}_i} = \frac{\mathrm{d}f}{\mathrm{d}\kappa_i}\frac{\mathrm{d}\kappa_i}{\mathrm{d}\bar{\kappa}_i} = \frac{\mathrm{d}f}{\mathrm{d}\kappa_i}\kappa_{s,i}. \tag{40}$$

In our algorithm the starting vector $\kappa^{(j=1)}$ is used for scaling. Additionally, a rescaling and a subsequent restart of the optimization process is preferable in the case of $\min\{|\kappa_i|\} > \mathrm{stol} \max\{|\kappa_i|\}$, where stol is some tolerance factor. In this case, the actual parameter set $\kappa^{(j)}$ is used as the scaling vector.

VI. NUMERICAL EXAMPLES

The model's equations of Table 1 have been incorporated into a computer program called *PARAGRAV(PARA*meter Identifikation mit Gradienten Verfahren). The basic flow chart of the program is according to Fig. 1, where either stress- or strain-controlled tests may be simulated. To account for possible stiffness of the ordinary equations, as mentioned before, a second-order midpoint rule is applied for integration. Optimization for the inverse problem can be performed with (1) a projection algorithm due to Bertsekas [1992]; (2) an SQP algorithm due to Schittkowski [1981]; (3) a one-level genetic algorithm due to Rechenberg (see Schwefel [1977]); or (4) a multilevel genetic algorithm due to Schwefel [1977].

In the subsequent sections numerical results are performed in the context of monotonic and cyclic uniaxial tension and compression tests. Optimization is performed with the multilevel genetic strategy and the Bertsekas algorithm. For the first method we used 3 parents and 20 descendants, while for the latter the BFGS matrix was used as an iteration matrix and the Gauss–Newton matrix (30) for preconditioning. The computer runs were performed on an IBM-250T.

VI.1 *Stability investigations for the inverse problem in case of the CHABOCHE model for monotonic and cyclic loading*

The goal of the simulations in this section is to assess the stability of parameter sets for the Chaboche model of Table 1 for the case of both monotonic and cyclic loading in a simulated experiment. For this purpose data for the stresses were generated for both cases based on strain-controlled experiments, with assumed parameters listed in the second column of Table 3. (Note, that no units are given for this purely numerical experiment.) The total time was $T = 100$ for monotonic loading, and $T = 1000$ was chosen in the second experiment, where we considered 10 cyclic loads. The time steps for both cases were chosen to be $t_k - t_{k-1} = 1$. The strain-controlled loading and the resulting curves for the stresses are shown in Figs 2 and 3, respectively.

As an objective function for the associated inverse problem in both cases the simple least-squares function

$$f(\kappa) = \frac{1}{2} \sum_{i_{dat}=1}^{n_{dat}} (\sigma_{i_{dat}}(\kappa) - \bar{\sigma}_{i_{dat}})^2 \tag{41}$$

is considered, where $n_{dat} = N = 100$ for the case of monotonic loading and $n_{dat} = N = 1000$ for the case of cyclic loading.

First, we want to verify Remark 3 of Section III.3 for the Chaboche case of monotonic loading. For this purpose, parameters of the third column of Table 3 are used for solution

Table 3. Assumed parameters for the Chaboche model. Note that all columns of parameter sets yield identical results for monotonic loading as shown in Fig. 2

n'	5·1	5·1	5·1
K'	70	70	70
b	0·2	0·4	1·0
q	60	40	10
c	0·4	0·2	1·2666E-4
γ	40	60	14229·74
k'	0	0	0

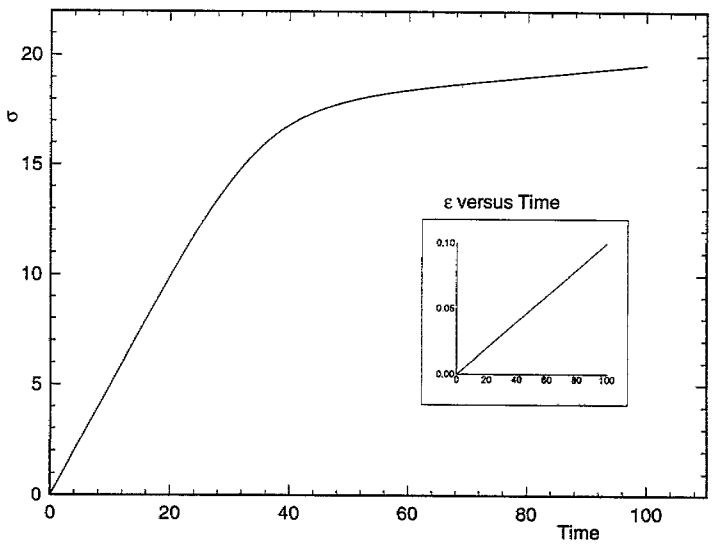

Fig. 2. Simulated data for the Chaboche model for monotonic loading.

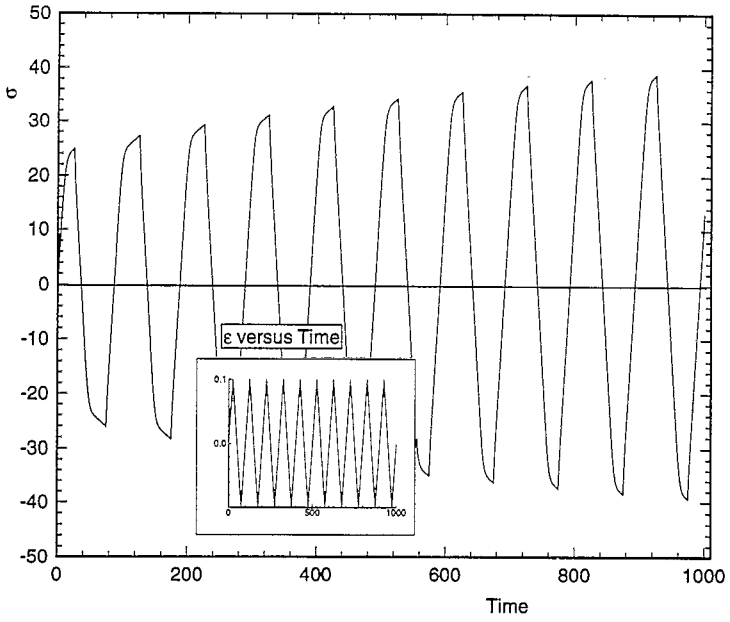

Fig. 3. Simulated data for the Chaboche model for cyclic loading.

of a direct problem. Note, that here the parameters b, c and q, γ of the second column have been interchanged. Then a solution of the corresponding direct problem with monotonic loading yields an identical response for the stresses as shown in Fig.2 as the parameters listed in the second column of Table 3. Further numerical tests (not reported here) based on minimizing the least-squares functional (41) showed that an infinite number of parameter sets can be generated, which give the same response for the stresses; for example, the fourth column of Table 4 also yields the results shown in Fig. 2.

The implications of the above linear dependencies within the direct problem for the numerical stability of the inverse problem become obvious by inspecting the eigenvalues and the eigenvectors of the Hessian of the least-squares functional (41). The eigenvalues are listed in the first column of Table 4. It can be observed that two values are close to zero, thus reflecting the appearance of two extra degrees of freedom for the parameter set and demonstrating the instable behaviour for solutions of problem (41) for the case of monotonic loading. In Table 5 the corresponding eigenvectors

Table 4. Eigenvalues for the Hessian of the least-squares functional in the case of parameters for the Chaboche model of the second column in Table 3

Monotonic loading	Cyclic loading
1·4535 +03	6·5608E+05
5·2677E+01	2·6746E+03
1·7936E−02	6·6404E+02
1·1115E−04	1·7299E−01
1·6150E−05	2·7647E−03
1·4201E−15	6·7722E−03
2·6768E−20	1·6326E−05

Table 5. Eigenvectors for the Hessian of the least-squares function in case of parameters for the Chaboche model of the second column in Table 3 and monotonic loading

n'	8·999E–01	–3·784E–01	–1·810E–01	–1·016E–01	6·289E–02	7·418E–07	–3·762E–10
K'	4·718E–02	–1·344E–02	–3·515E–01	7·407E–01	–5·704E–01	–7·685E–06	4·015E–09
b	2·151E–01	5·065E–01	–3·468E–02	4·957E–01	6·710E–01	2·008E–03	–1·565E–03
q	2·168E–03	5·126E–03	2·655E–04	–2·204E–03	–2·976E–03	6·255E–01	7·798E–01
c	3·251E–01	7·689E–01	3·958E–02	–3·274E–01	–4·407E–01	–8·109E–03	–2·069E–03
γ	1·088E–03	2·579E–03	2·866E–04	–2·903E–03	–3·928E–03	7·802E–01	–6·260E–01
k'	1·898E–01	–9·390E–02	9·170E–01	2·967E–01	–1·618E–01	–1·740E–06	8·642E–10

are listed. Inspection of the the sixth and seventh eigenvector, which form the (near-) null space of the Hessian, reveals, that basically the four parameters b, q, c, γ are responsible for the linear dependencies. This observation is in agreement with the results of Fig. 2, which are obtained with parameter sets according to Table 3.

In the third column of Table 4 the eigenvalues of the Hessian of the least-squares functional (41) corresponding to the simulation based on cyclic loading as shown in Fig. 3 are listed. As expected, now none of the eigenvalues is close to zero, thus indicating stability for solutions of the inverse problem.

VI.2 *Monotonic loading for High-Purity Aluminum Al 99.999*

The next example concerns parameter identification of the Bodner and Partom model of Table 1 in the case of high-purity aluminum Al 99.999. For this material, experimental data are available from Mecking [1989] for creep tests at several stress levels and at temperatures between 550 K and 700 K. The following results are concerned with the case at 550 K.

First, identification is based on the simple least-squares functional (8). Two computer runs were started using the Bertsekas algorithm with different starting vectors, as shown in Table 6. Additionally a genetic algorithm was used. From Table 6 it can be seen that the results obtained by the Bertsekas algorithm are identical. They differ from those obtained by using the genetic algorithm, which has a greater value for the objective function $f(\boldsymbol{\kappa})$. Note, that the Bertsekas algorithm discovered the value for D_0 in the expected range of Table 2 as proposed by Bodner [1987], which is not the case for the genetic algorithm. Furthermore, in Table 6 we compare the number of func-

Table 6. Starting and obtained values for the material parameters of the Bodner and Partom model for three different optimization runs. ITE and NFUNC denote the number of iterations and function evaluations, respectively

	Bertsekas, run 1		Bertsekas, run 2		Genetic algorithm	
	Starting	Solution	Starting	Solution	Starting	Solution
D_0 (1/s)	1·0 E–1	5·325 E+4	1·0 E+5	5·327 E+4	1·0 E–1	7·890 E–1
Z_0 (MPa)	1·0 E+2	1·857 E+3	1·0 E+5	1·857 E+3	1·0 E+2	1·0 E+2
Z_1 (MPa)	1·0 E+2	3·974 E+3	1·0 E+5	3·974 E+3	1·0 E+2	1·249 E+2
n'	5·0 E–1	1·270 E–1	5·0 E–2	1·270 E–1	5·0 E–1	2·720 E–1
m'	1·0 E+2	7·292 E+3	1·0 E+5	7·293 E+3	1·0 E+2	1·216 E+2
$f(\kappa)$	5·580 E+1	8·917 E–2	5·620 E+1	8·917 E–2	5·580 E+1	1·260 E–1
CPU [min]	32		30		1380	
ITE (NFUNC)	731(1058)		602(1065)		3003(42211)	

tion evaluations and the CPU time for the Bertsekas algorithm and the genetic algorithm. The great advantage of a gradient-based method is obvious.

In Fig. 4 it can be seen that the results of the simulation correspond well to the experimental data. However, these appearances are deceptive with regard to the stability. When considering the smallest eigenvalue of the Hessian $\mathbf{F}^*$ at the solution point, a value of 3.86×10^{-14} is obtained, thus indicating unstable results. This unreliability is also demonstrated when using perturbed data. In the third column of Table 7, results for the parameter set are reported in the case of a stochastic perturbation with a maximal value of 10% of each data ε_i, $i = 1, \ldots, n_{\text{dat}}$. A partially large deviation from the second column of Table 7 (which is recalled from Table 6) can be seen from this.

For this reason the numerical experiment is repeated with the regularized functional (9); that is, we combine the data information of Mecking [1989] and the model information of Bodner [1987] according to Table 2. The corresponding regularization

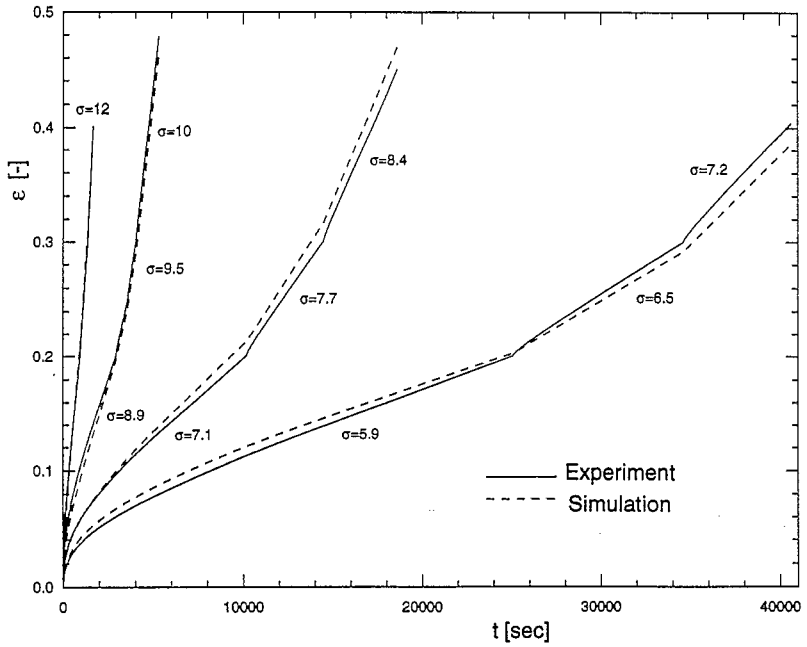

Fig. 4. Strains versus time for experimental data and Bodner and Partom simulated data for high-purity aluminum 99.9999. The stresses are given in MPa.

Table 7. Effect of perturbation of experimental data on solutions of parameter sets associated with a non-regularized and regularized least-squares functional. The second column is recalled from Table 6

Perturbed Regularized	No No	Yes No	No Yes	Yes Yes
D_0 (1/s)	5·325 E+4	1·474 E+5	1·001 E+4	1·001 E+4
Z_0 (MPa)	1·857 E+3	2·558 E+3	1·125 E+3	1·135 E+3
Z_1 (MPa)	3·974 E+3	5·468 E+3	2·352 E+3	2·351 E+3
n'	1·270 E–1	1·211 E–1	1·381 E–1	1·381 E–1
m'	7·292 E+3	1·005 E+4	4·324 E+3	4·323 E+3
$f_\delta(\kappa)$	8·917 E–2	2·937 E–1	8·995 E–2	2·941 E–1
$f_\mu(\kappa)$	—	—	5·991 E–4	5·992 E–4

parameters are as follows: for $\mathbf{B}_\delta$ the unity matrix is used; for $\mathbf{B}_\mu$ a diagonal matrix is chosen with elements 1.0; 0.1; 0.1; 0.1; 0.1; for $\bar{\kappa}$ we used values of the second column in Table 7 except for $\bar{\kappa} \equiv 10^4$; lastly, we set $\gamma = 10^{-8}$ for the total regularization term. The result of the minimization process is given in the fourth column of Table 7, with corresponding smallest eigenvalue of 9.54×10^{-9}. Note that the value for the least-squares functional is very close to that obtained in the second column. Let us mention that the same results were also obtained for different, arbitrary chosen, starting vectors. Next, the data are perturbed as described above, which gives the parameters listed in the fifth column of Table 7. These results with regularization indicate a greater robustness of the parameters with respect to perturbations.

To summarize, in an identification process for parameters of the Bodner and Partom model an *a priori* estimate for the parameter D_0 becomes necessary. This may be included as weighted model information into the basic least-squares functional. Alternatively, the value may also be kept constant during the identification process.

VI.3 *Monotonic loading at different temperatures for High-Purity Aluminum Al 99.999*

The next example is concerned with the same material as in the previous example; that is, high purity aluminum Al 99.999 is considered, based on experimental data from Mecking [1989]. Identification is performed for the Steck model of Table 1. In Mahnken and Stein [1994a] it was shown that in case of isothermal identification, a dependence of three parameters occurs. Thus, in order to identify the parameters without instabilities it is necessary to use data based on different temperature experiments. In our example, temperature will rise from 550 K to 650 K.

In the sequel, we make use of the relation $\bar{c}_i = \ln c_i$, $i = 1, 2$ for the parameters of Table 1, which can be viewed as a scaling procedure. The activation energy is $U_0 = 149$ kJ/mol, the gas constant is $R = 8.315 \times 10^{-3}$ kJ/(molK), and the elasticity modulus is $E = 1700$ MPa.

As in the previous example, the least-squares functional (8) is minimized with the Bertsekas algorithm and the genetic algorithm. In columns 3 and 5 of Table 8 the results of both optimization strategies are compared for the same starting values. It can be seen that the deviations at the solution point are drastic; however, the value for the objective function of the Bertsekas algorithm is lower. Furthermore, the execution time for the Bertsekas algorithm is much lower. Another run is performed with the Bertsekas algorithm (Run 2), where the solution vector obtained by the genetic algorithm is used as a starting vector. Then, in a comparatively short time (26 min), the same solution (column 7) as in Run 1 (column 3) is obtained. Let us note, that the minimal eigenvalue of the Hessian at the solution point is 3.33×10^{-4}, thus indicating stable results. The same conclusion can be drawn from the last column, which shows results from an optimization process based on 10% perturbed data (Run 3), and which show no drastic deviations from those of Run 1 or Run 2, respectively. Figure 5 depicts the strains for experiment and numerical simulation corresponding to Run 1 and Run 2, respectively.

VI.4 *Cyclic loading for AlMg*

In this example parameters for the Chaboche model of Table 1 are determined in the case of an aluminum/magnesium alloy. The underlying experimental data were obtained by Lange [1993]. The experiments were performed at room temperature for

Table 8. Starting and obtained values for the material parameters of the Steck model· ITE and NFUNC denote the number of iterations and function evaluations, respectively

	Bertsekas, run 1		*Genetic*		*Bertsekas, run 2*		*Bertsekas, run 3 (perturbed)*	
	Starting	Solution(κ^*_{Bert})	Starting	Solution(κ^*_{gen})	Starting	Solution	Starting	Solution
λ' (mol/kJ)	1·0 E–3	5·739 E–3	1·0 E–3	6·194 E–1			1·0 E–3	6·249 E–3
ΔV (kJ mm^2/N mol)	1·0 E+0	6·741 E–1	1·0 E+0	1·798 E+0			1·0 E+0	8·514 E–1
α	1·0 E+0	9·900 E–1	1·0 E+0	9·417 E–1			1·0 E+0	9·909 E–1
κ'	1·0 E+0	2·891 E–1	1·0 E+0	7·336 E–1	κ^*_{gen}	κ^*_{Bert}	1·0 E+0	3·286 E–1
$\bar{c}_1$(ln(kJ/mol s))	3·0 E+1	2·614 E+1	3·0 E+1	1·642 E+1			3·0 E+1	2·480 E+1
β	1·0 E+0	4·578 E+0	1·0 E+0	5·033 E+0			1·0 E+0	5·284 E+0
$\bar{c}_2$(ln(kJ/mol s))	3·0 E+1	1·547 E+1	3·0 E+1	3·062 E+1			3·0 E+1	1·426 E+1
$f(\kappa)$	6·880 E+4	9·454 E–3	6·880 E+4	5·469 E–2	5·469 E–2	9·454 E–3	6·880 E+4	9·454 E–3
CPU (min)	29		1260		26		26	
ITE (NFUNC)	1005 (1493)		2949 (58947)		874 (1297)		763 (1057)	

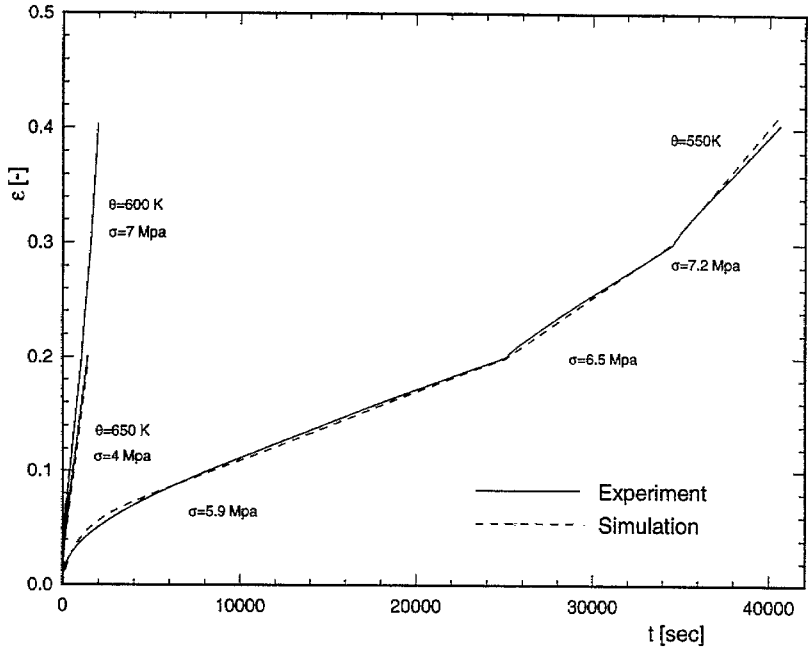

Fig. 5. Strains versus time for experimental data and Steck simulated data for high-purity aluminum 99.9999.

cylindrical hollow specimens with an outer radius of 28 mm and a thickness of 2 mm. The specimens were subjected to a periodic strain of an amplitude of $\varepsilon_{max} = 0.3\%$ at a strain rate of $\dot{\varepsilon} = 0.2\%\ s^{-1}$. A total of 110 cycles were generated during the test; however, experimental data are available only for 20 cycles. For Young's modulus we set $E = 1.09 \times 10^5$ MPa in the subsequent simulations.

As an objective function for the inverse problem the simple least-squares functional

$$f(\kappa) = \frac{1}{2} \| \sigma(\kappa) - \bar{\sigma} \|_2^2 \tag{42}$$

is minimized, which is the analogue of (8) for the case of strain-controlled experiments. Note that due to the incompleteness of the data set, $\bar{\sigma}$ contains data only at 20 cycles out of the total of 110. Again, minimization was performed with the Bertsekas algorithm and the genetic algorithm.

The starting vector and the solution vectors are given in Table 9. Concerning the Bertsekas algorithm three different runs were made. Run 1 and Run 2 were started with the vector in the second column; however, for Run 2 a regularization was performed analogously to (9). Here, for $\mathbf{B}_\delta$ and for $\mathbf{B}_\mu$ the unity matrix is chosen, $\bar{\kappa} = \kappa^{(j=0)}$ and we set $\gamma = 10^{-5}$. It can be seen that no convergence was attained for Run 1 after 2000 iteration steps, while minimization with the regularized functional attained convergence after 201 steps. The corresponding minimal eigenvalue of the Hessian at the solution point is 7.62×10^{-2}, which indicates stable results. This is also confirmed by Run 3, where each data was perturbed stochastically with a maximal value of 10%. (For this run no regularization was used, and the solution vector of Run 2 was used as a starting vector.) It can be seen that the effect of the perturbation is negligible.

In the last two columns of Table 9 results for the genetic algorithm are shown. It can be seen that after 897 iterations the results are still poor (Run 4). After 10256

Table 9. Starting and obtained values for the material parameters of the Chaboche model for AlMg in the case of different optimization strategies and least-squares functions. Concerning Run 3, see text. ITE and NFUNC denote the number of iterations and function evaluations, respectively

		Bertsekas			Genetic algorithm	
	Start	Run 1	Run 2	Run 3	Run 4	Run 5
n'	5·0 E+0	4·582 E+0	1·360 E+1	1·360 E+1	4·971 E+0	1·250 E+1
K' (MPa)	1·0 E+2	2·344 E+2	4·242 E+1	4·242 E+1	1·972 E+2	3·896 E+1
b'	1·0 E+2	5·195 E+0	4·824 E+0	4·824 E+0	5·115 E+0	5·068 E+0
q (MPa)	1·0 E+2	6·233 E+1	6·827 E+1	6·827 E+1	6·488 E+1	6·697 E+1
c	1·0 E+2	0·206 E–1	1·542 E+3	1·542 E+3	1·173 E+2	1·546 E+3
γ (MPa)	1·0 E+2	9·840 E+4	4·719 E+1	4·719 E+1	1·792 E+2	4·736 E+1
k' (MPa)	1·0 E+1	0·000 E+0	0·000 E+0	0·000 E+0	8·543 E–1	2·238 E0
$f(\kappa)$	3·491 E+5	9·620 E+3	2·135 E+3	3·335 E+3	8·936 E+3	2·135 E+3
$f_\mu(\kappa)$	—	—	–3·582 E–5	—	—	—
CPU (min)	—	192	24	—	1440	605 10^3
ITE (NFUNC)	—	2000(2072)	201(250)	—	897(17752)	10256(204932)
Remark	—	No convergence	Regularized	Perturbed	—	—

iterations and 168 h the value for the objective function is still above that obtained by the Bertsekas algorithm (Run 2) in 24 min.

In Fig. 6 the curves for the stresses of the simulated data for the starting parameter set $\kappa^{j=0}$ and the solution set κ^* for the first 18 out of 110 cycles are shown, and they are compared with the experimental data at 9 out of 20 cycles, where data are available. Figure 7 depicts the stresses versus strains for three different cycles for the solution vector of the material parameters. It can be seen that a very substantial agreement of experimental and simulated data is obtained, except for the first cycle where the model is not able to simulate the horizontal plateau. This explains the relatively high model error for the values of the objective function at the solution point in Table 9.

VII. SUMMARY AND CONCLUDING REMARKS

In this paper a unified strategy for parameter identification of viscoplastic models based on different conceptions is presented by minimizing a least-squares functional with gradient-based optimization methods. For this purpose the associative gradient is obtained *analytically*, and as a main result a *recursion formula* is obtained. For the computation it follows that the gradient can be determined *simultaneously* to the step-by-step computation of the direct problem. Comparative results with a genetic algorithm with respect to execution time clearly demonstrate the *efficiency* of our strategy. Furthermore, in an optimization run for the Chaboche model with an inadequate starting guess it was shown that convergence for the Bertsekas algorithm can be accelerated with comparatively small regularization.

Another conclusion is concerned with the *numerical stability* of the obtained parameters. As shown in an example for the Bodner and Partom model, good agreement between experimental data and simulated data is no indication for stability. Small perturbations of the data may lead to large deviations of the results. For this purpose the Hessian of the least-squares functional at the solution point is determined, and then an eigenvalue analysis yields information about the robustness of the results.

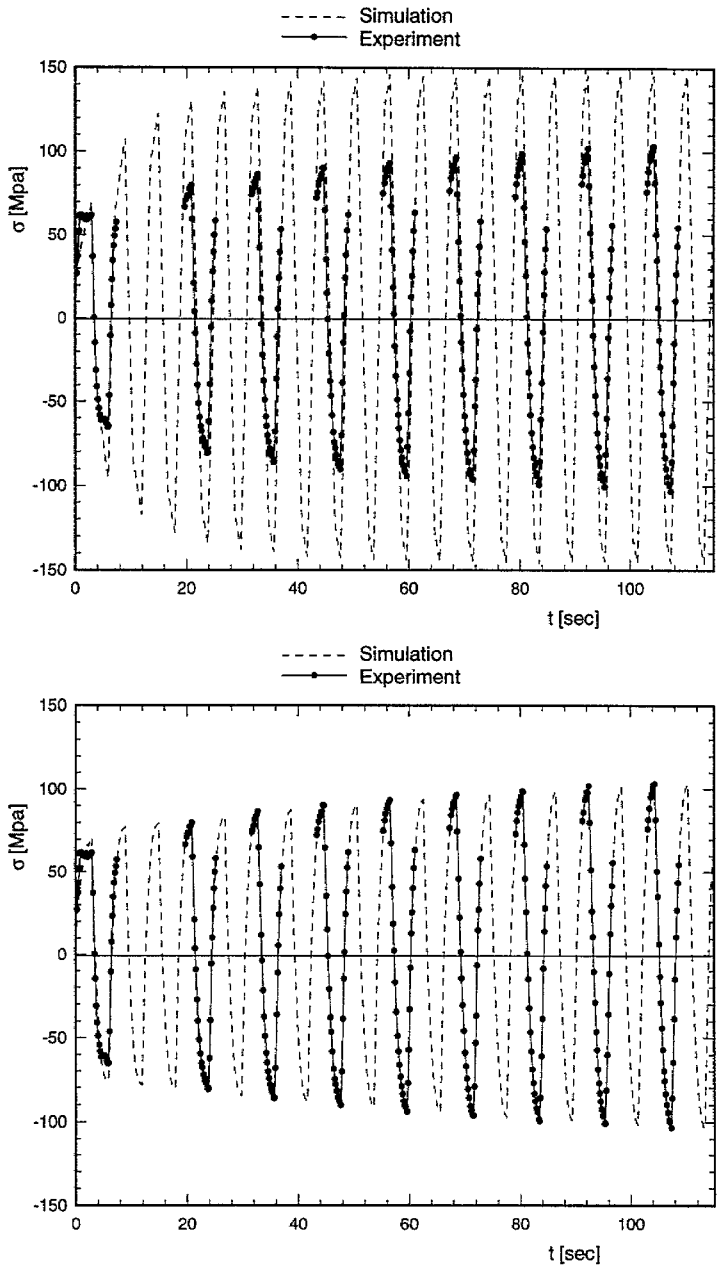

Fig. 6. Stresses versus time for the starting parameter set and the solution parameter set for the first 18 out of 110 cycles. Note the incompleteness of the experimental data set.

The cause of possible numerical instabilities may be twofold: first, the constitutive equations may have (too many) parameters, which yield (almost) linear dependencies within the model; secondly, the experiment may be inadequate in the sense that physical effects intended by the model are not properly activated. Consequently, if numerical instabilities are detected, the model and/or the experiment have to be revised.

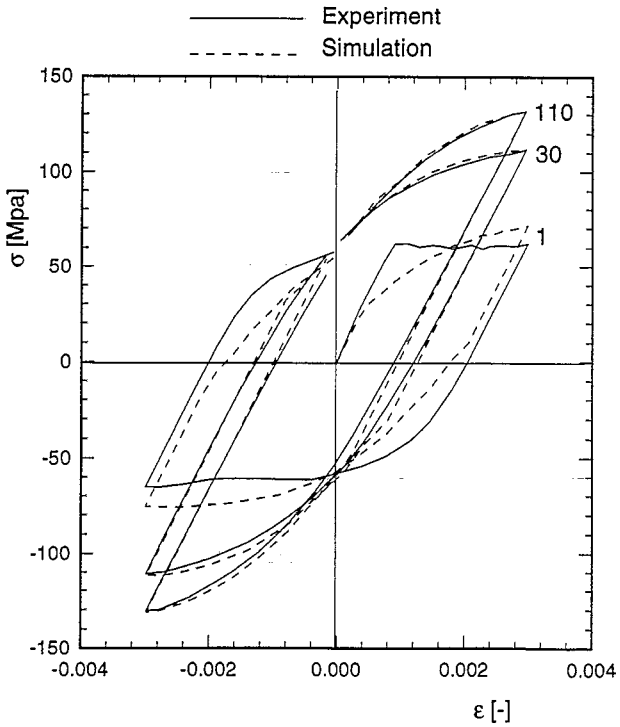

Fig. 7. Stresses versus strains for three different cycles. The numbers 1, 30 and 110 correspond to the specific cycles.

In particular, when identifying parameters for the three representative models of Table 1 at least the following guidelines are recommended, in order to achieve stability for the results of the inverse problem. For the Chaboche model at least cyclic experiments are necessary. Otherwise, in the case of monotonic loading, the identical structure for the linear and the kinematic hardening variable yields two extra degrees of freedom for the parameter set. For the Bodner and Partom model an *a priori* estimate for the parameter D_0 becomes necessary. This value is kept constant during the identification process or it may be included as weighted model information into the basic least-squares functional. Concerning the Steck model, we recall as a result from Mahnken and Stein [1994a], that the experiments have to be performed at different temperatures.

Let us make some remarks related to issues of future work in the field of parameter identification:

1. When using a deterministic optimization strategy based on gradient evaluations, it is not guaranteed that the global minimum of the problem is obtained. In our tests we tried several starting vectors and always obtained the same solution. However, a more systematic approach would be to use a hybrid method: that is, a combination of a deterministic and a stochastic strategy.

2. As mentioned before, numerical instabilities for the inverse problem can also be circumvented by using a regularized version of the basic least-squares function. In this respect the basic least-squares functional is enhanced by model information obtained

for example, by a mechanistic identification approach or by physical interpretation of some parameters. However, an extensive study on an optimal choice strategy for the regularization parameters is still open.

3. The effect of discretization errors (for example, in the context of a midpoint rule for time integration) on solution for the material parameters was not discussed in this paper. We still work on strategies in order to include adaptive procedures for the time-step selection in the context of the optimization procedure.

Acknowledgements—The authors would like to thank Professor J. Baumeister for several helpful suggestions, which have been included in this paper. This work was performed in the context of the German research network Sonderforschungsbereich 319 (SFB 319): "Stoffgesetze für das inelastische Verhalten metallischer Werkstoffe — Entwicklung und Anwendung". The support by the Deutsche Forschungsgemeinschaft (DFG) is gratefully acknowledged.

REFERENCES

1923 Hadamard. J., Lectures on Cauchy's Problem in Linear Partial Differential Equations. Yale University Press, New Haven.
1949 Prager, W., "Recent Developments in the Mathematical Theory of Plasticity," J. Appl. Phys., **15**, 22.
1974 Bard, Y., Nonlinear Parameter Estimation. Academic Press, New York.
1975 Bodner, S.R. and Partom, Y. "Constitutive Equations for Elastic-Viscoplastic Strain-Hardening Materials," Trans. ASME, J. Appl. Mech., **42**, 385–389.
1977 Chaboche, J.-L., "Viscoplastic Constitutive Equations for the Description of Cyclic and Anisotropic Behavior of Metals", Bull. Acad. Pol. Sci., Ser. Sci. Tech., **25**, 33.
1977 Powell, M.J.D., "A Fast Algorithm for Nonlinear Constrained Optimization Calculations," in Watson, G.A. (ed.), Numerical Analysis, Proc. of the Biennial Conf. (Dundee, June 1977) (Lecture Notes in Mathematics 630). Springer, Berlin.
1977 Schwefel, K.P., "Numerische Optimierung von Computer-Modellen mittels der Evolutionsstrategie. Birkhäuser, Basel.
1981 Gill, P.E., Murray, W. and Wright, M.H., Practical Optimization. Academic Press, London.
1981 Schittkowski, K., "The Nonlinear Programming Method of Wilson, Han and Powell with an Augmented Lagrangian Type Line Search Function," Numerische Mathematik, **38**(1), 83–114.
1982 Bertsekas, D.P., "Projected Newton Methods for Optimization Problems with Simple Constraints," SIAM J. Con. Opt., **20**(2), 221–246.
1983 Dennis, J.E. and Schnabel, R.B., Numerical Methods for Unconstrained Optimization and Nonlinear Equations. Prentice Hall, New Jersey.
1984 Luenberger D.G., Linear and Nonlinear Programming, 2nd edn. Addison- Wesley, Reading.
1984 Morozov, V.A., Methods for Solving Incorrectly Posed Problems," Springer, New York.
1984 Pugachew, V.S., Probability Theory and Mathematical Statistics for Engineers. Pergamon, Oxford.
1985 Steck, E.A., "A Stochastic Model for the High-Temperature Plasticity of Metals," Int. J. of Plast. **1**, 243–258.
1985 Swearengen, J.C. and Holbrook, J.H., "Internal Variable Models for Rate-Dependent Plasticity: Analysis of Theory and Experiments", Res Mechanica, **13**, 93–128.
1987 Baumeister, J., Stable Solution of Inverse Problems. Vieweg, Braunschweig.
1987 Bodner, S.R., "Review of Unified Elastic-Viscoplastic Theory," Chapter 6 in Miller [1987].
1987 Krieg, R.D., Swearengen, J.C. and Jones, W.B., "A Physically Based Internal Variable Model for Rate Dependent Plasticity," Chapter 5 in Miller [1987].
1987 Miller A.K. (Ed.), Unified Constitutive Equations for Creep and Plasticity. Elsevier Applied Science, London.
1988 Engeln-Müllges, G. and Reuter, F., Formelsammlung zur numerischen Mathematik mit Standard-FORTRAN 77 Programmen. BI-Wissenschaftsverlag, Mannheim.
1989 Banks, H.T. and Kunisch, K., Estimation Techniques for Distributed Parameter Systems. Birkhäuser, Boston.
1989 Louis, A.K., Inverse und Schlecht Gestellte Probleme. Teubner, Stuttgart.
1989 Mecking, H., "Bestimmung der Werkstoffparameter für das Kriechen von Aluminium Legierungen," Final Report for the DFG research project Me 428/7, Technical University Hamburg-Harburg.
1989 Müller, D. and Hartmann, G., "Identification of Material Parameters for Inelastic Constitutive Models Using Principles of Biologic Evolution," J. Eng. Mat. Tech. (ASME), **111**, 299–305.
1990 Lemaitre, J. and Chaboche, J.L., Mechanics of Solid Materials. Cambridge University Press, Cambridge.

1992 Huang, S. and Khan, A.S., "Modeling the Mechanical Behavior of 1100-0 Aluminum at Different Strain Rates by the Bodner-Partom Model," Int. J. Plast., **8**, 501–517.
1992 Kublik, F., "Vergleich zweier Werkstoffmodelle bei ein- und mehrachsigen Versuchs durchführungen im Hochtemperaturbereich," Dissertation, University of Braunschweig, Inst. f. Allg. Mech. u. Festigk.
1992 Kublik, F. and Steck, E.A., "Comparison of Two Constitutive Models with One- and Multiaxial Experiments," in D. Besdo and E. Stein (eds), IUTAM Symposium Hannover 1991, Finite Inelastic Deformations — Theory and Applications. Springer, Berlin.
1992 Mahnken, R., "Duale Verfahren für nichtlineare Optimierungsprobleme in der Strukturmechanik," Dissertation, Forschungs- und Seminarberichte aus dem Bereich der Mechanik der Universität Hannover, F 92 /3.
1992 Schlums, H. and Steck, E.A., "Description of Cyclic Deformation Process with a Stochastic Model for Inelastic Behaviour of Metals," Int. J. Plast., **8**, 147–159.
1993 Lange, G. "Veränderung des Werkstoffzustandes bei mehrachsiger plastischer Wechselbeanspruchung," Report of the German research network Sonderforschungsbereich 319: Stoffgesetze für das inelastische Verhalten metallischer Werkstoffe — Entwicklung und Anwendung. University of Braunschweig.
1993 Senseny, P.E., Brodsky, N.S. and De Vries, K.L., "Parameter Evaluation for a Unified Constitutive Model," Trans. ASME: J. Eng. Mat. Tech., **115**, 157–162.
1994a Mahnken, R. and Stein, E., "The Parameter-Identification for Visco-Plastic Models via Finite-Element-Methods and Gradient-Methods," Modelling Simul. Mater. Sci. Eng., **2**, 597–616.
1994b Mahnken, R. and Stein, E., "Gradient-Based Methods for Parameter Identification of Viscoplastic Materials," in H.D. Bui and M. Tanaka *et al.* (eds), Inverse Problems in Engineering Mechanics. A.A. Balkama, Rotterdam.

APPENDIX A: PARTIAL DERIVATIVES OF THE STATE EQUATIONS IN CASE OF THE BODNER AND PARTOM MODEL

It is the object of Appendix A to evaluate the partial derivatives of the state equation (17) for the Bodner and Partom model of Table 1. The following results are related to stress-controlled experiments. The extension to strain-controlled experiments is straightforward.

The vector of material parameters ($m = 5$) is defined as

$$\kappa := [D_0, Z_0, Z_1, n', m']^T \tag{A.1}$$

(A.1.) Implicit function

The implicit functions according to (15)–(16) are defined as

$$g_{k,1} := \varepsilon_k - \varepsilon_{k-1} - \Delta\varepsilon_k^{\text{in}} - \Delta\varepsilon_k^{\text{el}} \tag{A.2}$$

$$g_{k,2} := Z_k - Z_{k-1} - \Delta Z_k \tag{A.3}$$

where

$$\Delta\varepsilon_k^{\text{in}} := \frac{2}{\sqrt{3}}\Delta t_k D_0 \exp\left[-\frac{n'+1}{2n'}\frac{Z_{k-1/2}}{\sigma_{k-1/2}}\right] \tag{A.4}$$

$$\Delta Z_k := \frac{\sigma_{k-1/2} m'}{Z_0}(Z_1 - Z_{k-1/2})\Delta\varepsilon_k^{\text{in}} \tag{A.5}$$

$$\sigma_{k-1/2} = \frac{1}{2}(\sigma_k + \sigma_{k-1}) \tag{A.6}$$

$$Z_{k-1/2} = \frac{1}{2}(Z_k + Z_{k-1}) \tag{A.7}$$

(A.2.) Jacobian

The elements of the Jacobian (19) are given by

$$J_{k,11} = \frac{\partial g_{k,1}}{\partial \varepsilon_k} = 1 \tag{A.8}$$

$$J_{k,21} = \frac{\partial g_{k,1}}{\partial Z_k} = -\frac{\partial \Delta \varepsilon_k^{\text{in}}}{\partial Z_k} \tag{A.9}$$

$$J_{k,12} = \frac{\partial g_{k,2}}{\partial \varepsilon_k} = 0 \tag{A.10}$$

$$J_{k,22} = \frac{\partial g_{k,2}}{\partial Z_k} = 1 - \frac{\partial \Delta Z_k}{\partial Z_k} \tag{A.11}$$

where

$$\frac{\partial \Delta \varepsilon_k^{\text{in}}}{\partial \varepsilon_k} = 0 \tag{A.12}$$

$$\frac{\partial \Delta \varepsilon_k^{\text{in}}}{\partial Z_k} = -\Delta \varepsilon_k^{\text{in}}(n' + 1)\frac{Z_{k-1/2}}{\sigma_{k-1/2}}\frac{1}{2Z_{k-1/2}} \tag{A.13}$$

$$\frac{\partial \Delta Z_k}{\partial \varepsilon_k} = 0 \tag{A.14}$$

$$\frac{\partial \Delta Z_k}{\partial Z_k} = \frac{\Delta Z_k}{\Delta \varepsilon_k^{\text{in}}}\frac{\partial \Delta \varepsilon_k^{\text{in}}}{\partial Z_k} - \frac{1}{2}\Delta \varepsilon_k^{\text{in}}\frac{\sigma_{k-1/2} m'}{Z_0} \tag{A.15}$$

Consequently the inverse of $\mathbf{J}_k$ is

$$\mathbf{J}_k^{-1} = \begin{bmatrix} 1 & -\frac{J_{k,12}}{J_{k,22}} \\ 0 & -\frac{1}{J_{k,22}} \end{bmatrix}. \tag{A.16}$$

(A.3.) Derivatives with respect to the material parameters

The derivatives for $g_{k,1}$ are given by

$$\frac{\partial g_{k,2}}{\partial \kappa_i} = -\frac{\partial \Delta \varepsilon_k^{\text{in}}}{\partial \kappa_i}, \qquad i = 1, \ldots, 5 \tag{A.17}$$

where

$$\frac{\partial \Delta \varepsilon_k^{\text{in}}}{\partial \kappa_1} = \frac{\Delta \varepsilon_k^{\text{in}}}{D_0} \tag{A.18}$$

$$\frac{\partial \Delta \varepsilon_k^{\text{in}}}{\partial \kappa_i} = 0, \qquad i = 2, 3, 5 \tag{A.19}$$

$$\frac{\partial \Delta \varepsilon_k^{\text{in}}}{\partial \kappa_4} = -\Delta \varepsilon_k^{\text{in}} \frac{Z_{k-1/2}}{\sigma_{k-1/2}} \left[\left(-\frac{1}{2n'^2} \right) + \frac{n'+1}{2n'} \log \left(\left(\frac{Z_{k-1/2}}{\sigma_{k-1/2}} \right)^{2n'} \right) 2 \right] \tag{A.20}$$

whereas for $g_{k,2}$ we have

$$\frac{\partial g_{k,2}}{\partial \kappa_i} = -\frac{\partial \Delta Z_k}{\partial \kappa}, \qquad i = 1, \ldots, 5 \tag{A.21}$$

where

$$\frac{\partial \Delta Z_k}{\partial \kappa_i} = \frac{\Delta Z_k}{\Delta \varepsilon_k^{\text{in}}} \frac{\partial \Delta \varepsilon_k^{\text{in}}}{\partial \kappa_i}, \qquad i = 1, 4 \tag{A.22}$$

$$\frac{\partial \Delta Z_k}{\partial \kappa_2} = -\frac{\Delta Z_k}{Z_0} \tag{A.23}$$

$$\frac{\partial \Delta Z_k}{\partial \kappa_3} = \frac{\sigma_{k-1/2} m'}{Z_0} \Delta \varepsilon_k^{\text{in}} \tag{A.24}$$

$$\frac{\partial \Delta Z_k}{\partial \kappa_5} = \frac{\Delta Z_k}{m'}. \tag{A.25}$$

Since the initial value $Z(t = 0) = Z_0$ is regarded as a material parameter, additionally for the first step we need

$$\frac{\partial g_{k=1}^2}{\partial \kappa_2} = \frac{\partial}{\partial Z_0} (Z_{k=1} - Z_0 - \Delta Z_{k=1}) = -1 - \frac{\partial \Delta Z_{k=1}}{\partial \kappa_2}. \tag{A.26}$$

Since

$$\Delta Z_{k=1} = \frac{\sigma_{k-1/2} m'}{Z_0} \left(Z_1 - \frac{1}{2} (Z_{k=1} + Z_0) \right) \Delta \varepsilon_{k=1}^{\text{in}},$$

it follows that

$$\begin{matrix} \partial \Delta Z_{k=1} & 1 & \sigma_{k-1/2} m' & & \Delta Z_{k=1} & \partial \Delta \varepsilon_{k=1}^{\text{in}} \\ \partial Z_0 & 2 & Z_0 & & \Delta \varepsilon_{k=1}^{\text{in}} & \partial Z_0 \end{matrix} \tag{A.27}$$

Here we make the use of the relation

$$\frac{\partial \Delta \varepsilon_{k=1}^{\text{in}}}{\partial Z_0} = \frac{\partial \Delta \varepsilon_{k=1}^{\text{in}}}{\partial Z_{k=1}} = -J_{k=1,12} \tag{A.28}$$

The above relations are used in order to evaluate the recursion formula (26).

APPENDIX B: ON DETERMINATION OF THE HESSIAN OF THE LEAST-SQUARES FUNCTIONAL

It is the purpose of Appendix B to present a unified strategy for determination of the second derivative of the least-squares functional. As it will be seen, third-order matrices

will appear during the calculation. For this reason we will apply an index notation, contrary to the representation of Section IV.3 for the first derivative. Furthermore, contrary to the previous notation, we will use k as an upper index, which corresponds to the time step introduced in Section III.1. Using this notation, the sensitivity analysis for the first derivative is also briefly recalled in the subsequent analysis.

Considering the following least-squares function

$$f(\boldsymbol{\kappa}) = \frac{1}{2}\sum_{k=1}^{N} (\varepsilon^{(k)}(\boldsymbol{\kappa}) - \bar{\varepsilon}^{(k)})^2, \tag{B.1}$$

by use of the chain rule the gradient is given by

$$\frac{\mathrm{d}f(\boldsymbol{\kappa})}{\partial \kappa_i} = \sum_{k=1}^{N} (\varepsilon^{(k)}(\boldsymbol{\kappa}) - \bar{\varepsilon}^{(k)}) \frac{\mathrm{d}\varepsilon^{(k)}(\boldsymbol{\kappa})}{\partial \kappa_i}, \tag{B.2}$$

and for the Hessian we have

$$\frac{\mathrm{d}^2 f(\boldsymbol{\kappa})}{\partial \kappa_j \partial \kappa_i} = \sum_{k=1}^{N} \left(\frac{\mathrm{d}\varepsilon^{(k)}}{\mathrm{d}\kappa_i} \frac{\mathrm{d}\varepsilon^{(k)}}{\mathrm{d}\kappa_j} + (\varepsilon^{(k)}(\boldsymbol{\kappa}) - \bar{\varepsilon}^{(k)}) \frac{\mathrm{d}^2\varepsilon^{(k)}(\boldsymbol{\kappa})}{\mathrm{d}\kappa_j \mathrm{d}\kappa_i} \right), \tag{B.3}$$

where $i, j = 1, ..., m$. From (B.2) and (B.3) it can be seen, that basically $\mathrm{d}\varepsilon^{(k)}(\boldsymbol{\kappa})/\mathrm{d}\kappa_i$ and $\mathrm{d}^2\varepsilon^{(k)}(\boldsymbol{\kappa})/\mathrm{d}\kappa_j \mathrm{d}\kappa_i$ are required. For this purpose we will calculate $\mathrm{d}Y_l^{(k)}/\mathrm{d}\kappa_i$ and $\mathrm{d}^2 Y_l^{(k)}/\mathrm{d}\kappa_i \mathrm{d}\kappa_j$, where $Y_1^{(k)} := \varepsilon^{(k)}$, $Y_l^{(k)} := q_{l-1}^{(k)}$, $l = 2 ..., n_q$.

As in Section IV.3 the point of departure is the state equation, which is regarded as an implicit function:

$$G_r = G_r(\boldsymbol{\kappa}, \mathbf{Y}^{(k)}(\boldsymbol{\kappa}), \mathbf{Y}^{(k-1)}(\boldsymbol{\kappa})), \tag{B.4}$$

where $r = 1, ..., n_q + 1$. In calculating the total differential

$$\frac{\mathrm{d}G_r}{\mathrm{d}\kappa_i} = \frac{\partial G_r}{\partial \kappa_i} + \frac{\partial G_r}{\partial Y_l^{(k)}} \frac{\mathrm{d}Y_l^{(k)}}{\mathrm{d}\kappa_i} + \frac{\partial G_r}{\partial Y_l^{(k-1)}} \frac{\mathrm{d}Y_l^{(k-1)}}{\mathrm{d}\kappa_i} = 0 \tag{B.5}$$

and introducing a matrix with elements D_{mr}, which satisfy

$$D_{mr} \frac{\partial G_r}{\partial Y_l^{(k)}} = \delta_{ml}, \tag{B.6}$$

$m = 1, ..., n_q + 1$, we can solve for the unknowns

$$\frac{\mathrm{d}Y_m^{(k)}}{\mathrm{d}\kappa_i} = -D_{mr} \left(\frac{\partial G_r}{\partial \kappa_i} + \frac{\partial G_r}{\partial Y_l^{(k-1)}} \frac{\mathrm{d}Y_l^{(k-1)}}{\mathrm{d}\kappa_i} \right) . \tag{B.7}$$

Next, a second total differential is introduced, where it has to be taken into account, that $\partial G_r/\partial \kappa_i$, $\partial G_r/\partial Y_l^{(k)}$, $\partial G_r/\partial Y_l^{(k-1)}$ are dependent on $\boldsymbol{\kappa}$, $\mathbf{Y}^{(k)}(\boldsymbol{\kappa})$, $\mathbf{Y}^{(k-1)}(\boldsymbol{\kappa})$. We obtain

$$\begin{aligned}
\frac{\mathrm{d}G_r}{\mathrm{d}\kappa_j \mathrm{d}\kappa_i} = {} & \frac{\partial^2 G_r}{\partial \kappa_j \partial \kappa_i} + \frac{\partial^2 G_r}{\partial Y_l^{(k)} \partial \kappa_i} \frac{\mathrm{d}Y_l^{(k)}}{\mathrm{d}\kappa_j} + \frac{\partial^2 G_r}{\partial Y_l^{(k-1)} \partial \kappa_i} \frac{\mathrm{d}Y_l^{(k-1)}}{\mathrm{d}\kappa_j} \\
& + \left(\frac{\partial^2 G_r}{\partial \kappa_j \partial Y_l^{(k)}} + \frac{\partial^2 G_r}{\partial Y_m^{(k)} \partial Y_l^{(k)}} \frac{\mathrm{d}Y_m^{(k)}}{\mathrm{d}\kappa_j} + \frac{\partial^2 G_r}{\partial Y_m^{(k-1)} \partial Y_l^{(k)}} \frac{\mathrm{d}Y_m^{(k-1)}}{\mathrm{d}\kappa_j} \right) \frac{\mathrm{d}Y_l^{(k)}}{\mathrm{d}\kappa_i} \\
& + \frac{\partial G_r}{\partial Y_l^{(k)}} \frac{\mathrm{d}^2 Y_l^{(k)}}{\mathrm{d}\kappa_j \mathrm{d}\kappa_i}
\end{aligned}$$

$$+\left(\frac{\partial^2 G_r}{\partial \kappa_j \partial Y_l^{(k-1)}}+\frac{\partial^2 G_r}{\partial Y_m^{(k)} \partial Y_l^{(k-1)}}\frac{\mathrm{d}Y_m^{(k)}}{\mathrm{d}\kappa_j}+\frac{\partial^2 G_r}{\partial Y_m^{(k-1)} \partial Y_l^{(k-1)}}\frac{\mathrm{d}Y_m^{(k-1)}}{\mathrm{d}\kappa_j}\right)\frac{\mathrm{d}Y_l^{(k-1)}}{\mathrm{d}\kappa_i}$$

$$+\frac{\partial G_r}{\partial Y_l^{(k-1)}}\frac{\mathrm{d}^2 Y_l^{(k-1)}}{\mathrm{d}\kappa_j \mathrm{d}\kappa_i}. \tag{B.8}$$

According to (27), the following relation holds

$$\frac{\partial}{\partial x}\left(\frac{\partial G_r}{\partial Y_l^{(k-1)}}\right)=\frac{\partial}{\partial x}\left(\frac{\partial G_r}{\partial Y_l^{(k)}}-2\delta_{kl}\right)=\frac{\partial^2 G_r}{\partial x \partial Y_l^{(k)}}, \tag{B.9}$$

and, consequently, it follows

$$\frac{\mathrm{d}G_r}{\mathrm{d}\kappa_j \mathrm{d}\kappa_i}=\frac{\partial^2 G_r}{\partial \kappa_j \partial \kappa_i}+\frac{\partial G_r}{\partial Y_l^{(k-1)}}\frac{\mathrm{d}^2 Y_l^{(k-1)}}{\mathrm{d}\kappa_j \mathrm{d}\kappa_i}$$

$$+\frac{\partial^2 G_r}{\partial Y_j^{(k)} \partial \kappa_i}\left(\frac{\mathrm{d}Y_l^{(k)}}{\mathrm{d}\kappa_j}+\frac{\mathrm{d}Y_l^{(k-1)}}{\mathrm{d}\kappa_j}\right)+\frac{\partial^2 G_r}{\partial Y_j^{(k)} \partial \kappa_i}\left(\frac{\mathrm{d}Y_l^{(k)}}{\mathrm{d}\kappa_i}+\frac{\mathrm{d}Y_l^{(k-1)}}{\mathrm{d}\kappa_i}\right)$$

$$+\frac{\partial^2 G_r}{\partial Y_m^{(k)} \partial Y_l^{(k)}}\left(\frac{\mathrm{d}Y_m^{(k)}}{\mathrm{d}\kappa_j}+\frac{\mathrm{d}Y_m^{(k-1)}}{\mathrm{d}\kappa_j}\right)\left(\frac{\mathrm{d}Y_l^{(k)}}{\mathrm{d}\kappa_i}+\frac{\mathrm{d}Y_l^{(k-1)}}{\mathrm{d}\kappa_i}\right)$$

$$+\frac{\partial G_r}{\partial Y_l^{(k)}}\frac{\mathrm{d}^2 Y_l^{(k)}}{\mathrm{d}\kappa_j \mathrm{d}\kappa_i}. \tag{B.10}$$

Analogously to the determination of the first derivative, the above equation can be solved for the unknowns:

$$\frac{\mathrm{d}^2 Y_m^{(k)}}{\mathrm{d}\kappa_i \mathrm{d}\kappa_j}=-D_{mr}\left(\frac{\partial^2 G_r}{\partial \kappa_j \partial \kappa_i}+\frac{\partial G_r}{\mathrm{d}Y_l^{(k-1)}}\frac{\mathrm{d}^2 Y_l^{(k-1)}}{\mathrm{d}\kappa_j \mathrm{d}\kappa_i}\right.$$

$$+\frac{\partial^2 G_r}{\partial Y_j^{(k)} \partial \kappa_i}\left(\frac{\mathrm{d}Y_l^{(k)}}{\mathrm{d}\kappa_j}+\frac{\mathrm{d}Y_l^{(k-1)}}{\mathrm{d}\kappa_j}\right)+\frac{\partial^2 G_r}{\partial Y_j^{(k)} \partial \kappa_i}\left(\frac{\mathrm{d}Y_l^{(k)}}{\mathrm{d}\kappa_i}+\frac{\mathrm{d}Y_l^{(k-1)}}{\mathrm{d}\kappa_i}\right)$$

$$\left.+\frac{\partial^2 G_r}{\partial Y_m^{(k)} \partial Y_l^{(k)}}\left(\frac{\mathrm{d}Y_m^{(k)}}{\mathrm{d}\kappa_j}+\frac{\mathrm{d}Y_m^{(k-1)}}{\mathrm{d}\kappa_j}\right)\left(\frac{\mathrm{d}Y_l^{(k)}}{\mathrm{d}\kappa_i}+\frac{\mathrm{d}Y_l^{(k-1)}}{\mathrm{d}\kappa_i}\right)\right) \tag{B.11}$$

Remarks

- Equation (B.11) shows that analogously to the first derivative a recursion formula is obtained.
- In order to solve (B.11), additionally to the first derivative, one has to determine $\partial^2 G_r/\partial \kappa_j \mathrm{d}\kappa_i$, $\partial^2 G_r/\partial Y_l \partial \kappa_i$, $\partial^2 G_r/\partial Y_l \partial Y_m$. These terms have to be provided separately for each material law, analogously as for the first derivative in Appendix A.